No. 246
November 1982

BUCKLING OF RISERS IN TENSION

DUE TO INTERNAL PRESSURE

by

Michael M. Bernitsas
Theodore Kokkinis

Prepared under contract for the
American Bureau of Shipping

Department of Naval Architecture
and Marine Engineering
College of Engineering
The University of Michigan
Ann Arbor, Michigan 48109

ensm

UMR1116

ABSTRACT

The global Euler buckling loads of marine risers and columns have been presented in an earlier report [5]. In this work we use these results to prove that risers which are in tension along their entire length may globally buckle as Euler columns due to internal static fluid pressure. Numerical examples are used to

1. demonstrate that this phenomenon may occur during normal operating conditions,

2. show the proper distribution of riser supporting forces between top tension and buoyancy,

3. illustrate the effect of boundary conditions on the occurrence of this phenomenon, and

4. study the effect of the riser geometric particulars, internal fluid static pressure and total buoyancy on the riser critical length at which buckling in tension may occur due to internal pressure.

ACKNOWLEDGEMENTS

This report is part of the outcome of the research on global elastic stability of risers carried out by the authors for the American Bureau of Shipping at the Department of Naval Architecture and Marine Engineering of the University of Michigan in Ann Arbor. The support of the Ocean Engineering Division of the American Bureau of Shipping is gratefully acknowledged.

CONTENTS

LIST OF FIGURES

Figure page

NOMENCLATURE

Ai	Airy Function of the first kind
Bi	Airy function of the second kind
B_m	Net buoyancy of buoyancy modules per unit length
B_w	Displaced weight of water by a unit length of riser
C_B, C_T	Linear restoring spring stiffness at bottom and top of riser respectively
D_i, D_o	Inner and outer riser diameters respectively
E	Young's Modulus
h_m	Free surface ordinate of drilling mud
h_w	Free surface ordinate of water
I	Moment of inertia of cross-sectional area
L	Length of riser
L*	Critical L for buckling in tension
p	Dimensionless vertical coordinate along the riser
P_e	Effective tension in the riser
r_B, r_T	Linear rotational spring stiffness at bottom and top of riser respectively
T	Actual tension in the riser
TTR	Tension at the top of the riser
U	Lateral displacement of riser
W_e	Effective weight of riser per unit length
W_m	Weight per unit length of fluid inside the riser
W_{st}	Weight of riser per unit length
z	Vertical coordinate along the riser

Greek Letters

β	Dimensionless W_e
β^*	Critical β for buckling in tension
δ	Dimensionless TTR
δ_{crit}	Dimensionless critical TTR
η	Ratio of apparent to effective riser weight
ρ_m	Drilling mud mass density
ρ_{st}	Mass density of steel
ρ_w	Mass density of water
τ	Dimensionless effective overpull at the lower end of the riser
τ_{crit}	Dimensionless critical effective overpull at the lower end of the riser

INTRODUCTION AND OUTLINE

The objective of this work is to prove that open ended tubular columns may buckle globally as Euler columns due to the action of internal fluid static pressure even while they are in tension along their entire length. Risers, columns, legs of Tension Leg Platforms and hydraulic columns are therefore prone to such instability. The eigenvalue problem which yields the riser stability boundaries has been formulated and solved in previous work [5]. In this work the results derived in [5] are used to prove this phenomenon and illustrate it numerically for various boundary conditions, geometric configurations and loading conditions.

Several aspects of this and related problems have been studied during the past forty years. In chronological order the following work has been done. Willers has calculated the asymptotic behavior of very long columns, with movably hinged lower end and with nonmovable ends, subject to their own weight and compressive end load [22]. Biezeno and Koch studied the stability of closed vertical tubes fully or partially submerged in water with or without internal fluid and concluded that buckling cannot occur [12]. This is expected since they considered closed tubes. Lubinski analyzed the buckling of drill strings inside marine drilling risers without end load or internal fluid pressure [17]. Duncan formulated the problem of instability of multiply and continuously loaded columns but scaled all loads in order to reduce the loading variables to one only [13]. Huang and Dareing calculated the natural frequencies and buckling loads of columns submerged in water for various boundary conditions [15,16]. Plunkett computed the asymptotic behavior of buckling loads of drill strings under their own weight and verified Willers' results using a different method [19]. Sugiyama and Ashida solved the problem of

buckling of columns under their own weight for various boundary conditions using a power series solution [21]. Sherman and Erzurumlu studied the effect of various loads on the static instability of circular tubular columns [20]. Bernitsas et al have computed the buckling loads, for the general eigenvalue problem described above, for the entire range of practical interest and eight different sets of boundary conditions that are considered of practical importance [5]. The phenomenon which is studied in this paper is similar in many respects to that observed by Goodman and Breslin namely, that unsupported vertical cables which are heavier than water may be sustained by the external hydrostatic pressure and not collapse [14].

In this report the formulation and solution of the problem is briefly presented in Chapter I and reference to published results is made. In Chapter II it is shown theoretically that risers which are in tension along their entire length may buckle globally as Euler columns due to internal fluid static pressure. This phenomenon is illustrated with numerical examples which show the proper distribution of the riser supporting forces between top tension and buoyancy and that this phenomenon may occur during regular operating conditions. In Chapter III the critical length, for which a riser of given configuration and loading condition may buckle in tension, is defined, calculated and plotted versus the loading condition for the eight sets of boundary conditions which are considered of practical importance [5]. In Chapter IV the riser critical length is compared for the four sets of boundary condition of risers with nonmovable supports. Finally in Chapter V similar comparisons are carried out for risers with movable supports.

I. PROBLEM FORMULATION AND SOLUTION

The eigenvalue problem described in the Introduction has been formulated and solved in reference [5]. In this chapter we briefly present the formulation and solution for the sake of completeness of this report.

I.1. Eigenvalue Problem

In dimensionless form the differential equation for the Euler global buckling analysis for a uniform riser is [5]:

$$\frac{d^4U}{dp^4} - (\beta p + \tau)\frac{d^2U}{dp^2} - \beta\frac{dU}{dp} = 0 \quad , \tag{I-1}$$

where

$$\beta = \frac{W_e L^3}{EI} \tag{I-2}$$

is the dimensionless effective weight per unit length,

$$\tau = \frac{P_e(0) L^3}{EI} \tag{I-3}$$

is the dimensionless effective tension at the lower end of the riser,

$$p = \frac{z}{L} \tag{I-4}$$

is the dimensionless coordinate along the riser,

$$W_e = W_{st} + W_m - B_w - B_m \quad , \tag{I-5}$$

$$W_{st} = \rho_{st} g \frac{\pi}{4} (D_o^2 - D_i^2) \quad , \tag{I-6}$$

$$W_m = \rho_m g \frac{\pi}{4} D_i^2 \quad , \tag{I-7}$$

$$B_w = \rho_w g \frac{\pi}{4} D_o^2 \quad , \tag{I-8}$$

$$\frac{dP_e(z)}{dz} = W_e \tag{I-9}$$

$$P_e(z) \equiv T(z) + \rho_w g \frac{\pi D_o^2}{4} (h_w - z) - \rho_m g \frac{\pi D_i^2}{4} (h_m - z) \quad , \tag{I-10}$$

and $$I = \frac{\pi}{64} (D_o^4 - D_i^4)$$

The rest of the symbols in the above equations are defined in the Nomenclature.

The general boundary conditions for a riser with rotational and linear springs at both ends are:

at the lower end where $p = 0$

$$\frac{EI}{L^3} \frac{d^3U(0)}{dp^3} - \frac{T(0)}{L} \frac{dU(0)}{dp} + C_B U(0) = 0 \tag{I-11}$$

and

$$\frac{EI}{L^2} \frac{d^2U(0)}{dp^2} + \frac{r_B}{L} \frac{dU(0)}{dp} = 0 \tag{I-12}$$

where C_B and r_B are the linear and rotational spring constants at the riser bottom respectively, and at the top of the riser where $p = 1$

$$\frac{EI}{L^3} \frac{d^3U(1)}{dp^3} - \frac{T(1)}{L} \frac{dU(1)}{dp} - C_T U(1) = 0 \tag{I-13}$$

and

$$\frac{EI}{L^2} \frac{d^2U(1)}{dp^2} - \frac{r_T}{L} \frac{dU(1)}{dp} = 0 \tag{I-14}$$

where C_T , r_T are the linear and rotational spring constants at the riser top respectively.

Equations (I-1) and (I-11) to (I-14) constitute an eigenvalue problem the eigenvalues of which define the riser stability boundary in the β-τ plane.

In this work eight sets of boundary conditions which are considered of practical importance are studied. Movable and nonmovable top supports are considered. The former are more appropriate for modelling risers and the latter for modelling regular columns. All conditions can be derived from the general equations (I-11) to (I-14) by setting the linear and rotational spring stiffness equal to 0 or ∞.

For risers (or columns) with nonmovable lower and upper boundaries the conditions become

$$U(0) = 0 \qquad \text{(I-15)} \qquad \text{and} \qquad U(1) = 0 \qquad \text{(I-16)}$$

in all cases and

1. for hinged-hinged risers

$$\frac{d^2U(0)}{dp^2} = 0 \qquad \text{(I-17)} \qquad \text{and} \qquad \frac{d^2U(1)}{dp^2} = 0 \qquad \text{(I-18)}$$

2. for clamped-hinged risers

$$\frac{dU(0)}{dp} = 0 \qquad \text{(I-19)} \qquad \text{and} \qquad \frac{d^2U(1)}{dp^2} = 0 \qquad \text{(I-20)}$$

3. for hinged-clamped risers

$$\frac{d^2U(0)}{dp^2} = 0 \qquad \text{(I-21)} \qquad \text{and} \qquad \frac{dU(1)}{dp} = 0 \qquad \text{(I-22)}$$

4. for clamped-clamped risers

$$\frac{dU(0)}{dp} = 0 \qquad \text{(I-23)} \qquad \text{and} \qquad \frac{dU(1)}{dp} = 0 \qquad \text{(I-24)}$$

For risers (or columns) with nonmovable lower boundary and movable upper boundary we have in all cases

$$U(0) = 0 \qquad \text{(I-25)}$$

and

5. for hinged-movably hinged risers

$$\frac{d^2U(0)}{dp^2} = 0 \qquad \text{(I-26)} \qquad\qquad \frac{d^2U(1)}{dp^2} = 0 \qquad \text{(I-27)}$$

and $$\frac{d^3U(1)}{dp^3} - (\beta + \tau)\frac{dU(1)}{dp} = 0 \qquad \text{(I-28)}$$

6. for clamped-movably hinged risers

$$\frac{dU(0)}{dp} = 0 \qquad \text{(I-29)} \qquad\qquad \frac{d^2U(1)}{dp^2} = 0 \qquad \text{(I-30)}$$

and $$\frac{d^3U(1)}{dp^3} - (\beta + \tau)\frac{dU(1)}{dp} = 0 \qquad \text{(I-31)}$$

7. for hinged-movably clamped risers

$$\frac{d^2U(0)}{dp^2} = 0 \qquad \text{(I-32)} \qquad\qquad \frac{dU(1)}{dp} = 0 \qquad \text{(I-33)}$$

and $$\frac{d^3U(1)}{dp^3} = 0 \qquad \text{(I-34)}$$

8. and for clamped-movably clamped risers

$$\frac{d^2U(0)}{dp^2} = 0 \qquad \text{(I-35)} \qquad\qquad \frac{dU(1)}{dp} = 0 \qquad \text{(I-36)}$$

and $$\frac{d^3U(1)}{dp^3} = 0 \qquad \text{(I-37)}$$

I.2. Solution

Two methods of numerical solution have been developed for these eigenvalue problems [5]. The first method is based on a closed form solution in terms of Airy functions of the first and second kind [4] which is given by equation (I-38)

$$U(p) = \beta^{-1/3} \{c_1' U_1(x) + c_2' U_2(x) + c_3' U_3(x) + c_4'\} \qquad \text{(I-38)}$$

where c_1' , c_2' , c_3' and c_4' are constants of integration

$$U_1(x) = \int^x \mathrm{Ai}(\zeta)\, d\zeta \qquad \text{(I-39)} \quad , \qquad U_2(x) = \int^x \mathrm{Bi}(\zeta)\, d\zeta \quad , \qquad \text{(I-40)}$$

$$U_3(x) = -\int^x \mathrm{Ai}(\zeta) \int^\zeta \mathrm{Bi}(\eta)\, d\eta d\zeta + \int^x \mathrm{Bi}(\zeta) \int^\zeta \mathrm{Ai}(\eta)\, d\eta d\zeta \quad , \qquad \text{(I-41)}$$

and $$x = \beta^{1/3} p + \beta^{-2/3} \tau \quad . \qquad \text{(I-42)}$$

The second method is based on a power series solution of the form [4]

$$U(p) = \sum_{n=1}^{\infty} a_n p^{n-1} \qquad \text{(I-43)}$$

Numerically neither method is stable over the entire domain of practical interest. The combined results of the two methods yield the eigenvalues in the β-τ plane up to the range of high β values where the asymptotic behavior of the stability boundaries can be derived analytically [9].

The results of the numerical implementation of these two methods are presented in report [5] in the form of stability boundaries in the β-τ plane for the first six buckling modes for each one of the eight sets of boundary conditions. Both linear and logarithmic scale graphs are used since the former better depict the low β riser behavior and the latter better do so for the high β behavior. Some of these results are used in this work to show that risers which are in tension along their entire length may buckle globally as Euler columns due to internal pressure.

II. BUCKLING OF RISERS IN TENSION DUE TO INTERNAL PRESSURE

The results derived in the previous chapter and published in references [5] and [9] are used in this chapter to prove that internal pressure may destabilize even short risers in tension.

II.1. Buckling in Tension

Buckling of a riser may occur if

$$\tau \leq \tau_{crit} \tag{II-1}$$

or equivalently if

$$P_e(0) \leq P_{e_{crit}}(0) \tag{II-2}$$

Using the definition of $P_e(0)$, given by equation (I-10), we can write (II-2) as

$$T(0) + (B_w - W_m)L \leq P_{e_{crit}}(0) \quad . \tag{II-3}$$

For $T(0) > 0$, and a partially buoyed riser, which is usually the case in practice, $T(z)$ is greater than zero for all values of z. Consequently, a riser may buckle even if the actual tension is positive along its entire length, if the following inequality holds

$$(B_w - W_m)L \leq T(0) + (B_w - W_m)L \leq P_{e_{crit}}(0) \quad . \tag{II-4}$$

This inequality can be satisfied even for moderate values of W_m, the weight of the drilling fluid per unit length of riser. This observation is very important for the computation of TTR. Equations (I-9) and (I-10) can be used to compute TTR for risers with properties independent of z. Since

$$TTR = T(L) \quad , \tag{II-5}$$

$$T(z) = T(0) + (W_{st} - B_m)z \quad , \tag{II-6}$$

and by definition

$$P_e(0) = T(0) + (B_w - W_m)L \quad , \tag{II-7}$$

we have

$$TTR = P_e(0) + W_e L \quad . \tag{II-8}$$

In dimensionless form equation (II-8) becomes

$$\delta = \tau + \beta \tag{II-9}$$

where $$\delta = \frac{TTR\ L^2}{EI} \quad . \tag{II-10}$$

More general expressions for TTR , for risers with properties varying with z , are derived in reference [7].

According to equations (II-5) and (II-6) to achieve positive $T(0)$ we must satisfy inequality (II-11)

$$TTR \geq (W_{st} - B_m)L \quad . \tag{II-11}$$

In dimensionless form (II-11) becomes

$$\delta \geq \eta\beta \tag{II-12}$$

where

$$\eta = \frac{W_{st} - B_m}{W_e} \quad . \tag{II-13}$$

η is the ratio of the apparent riser weight in water to the effective riser weight.

Consequently buckling in tension will occur if

$$\eta\beta \leq \delta < \tau_{crit} + \beta = \delta_{crit} \quad . \tag{II-14}$$

This region is marked by R in Figure 1 and is confined between line [DCR] which represents the dimensionless critical top tension, δ_{crit} , and line [1] which represents the first inequality in (II-14).

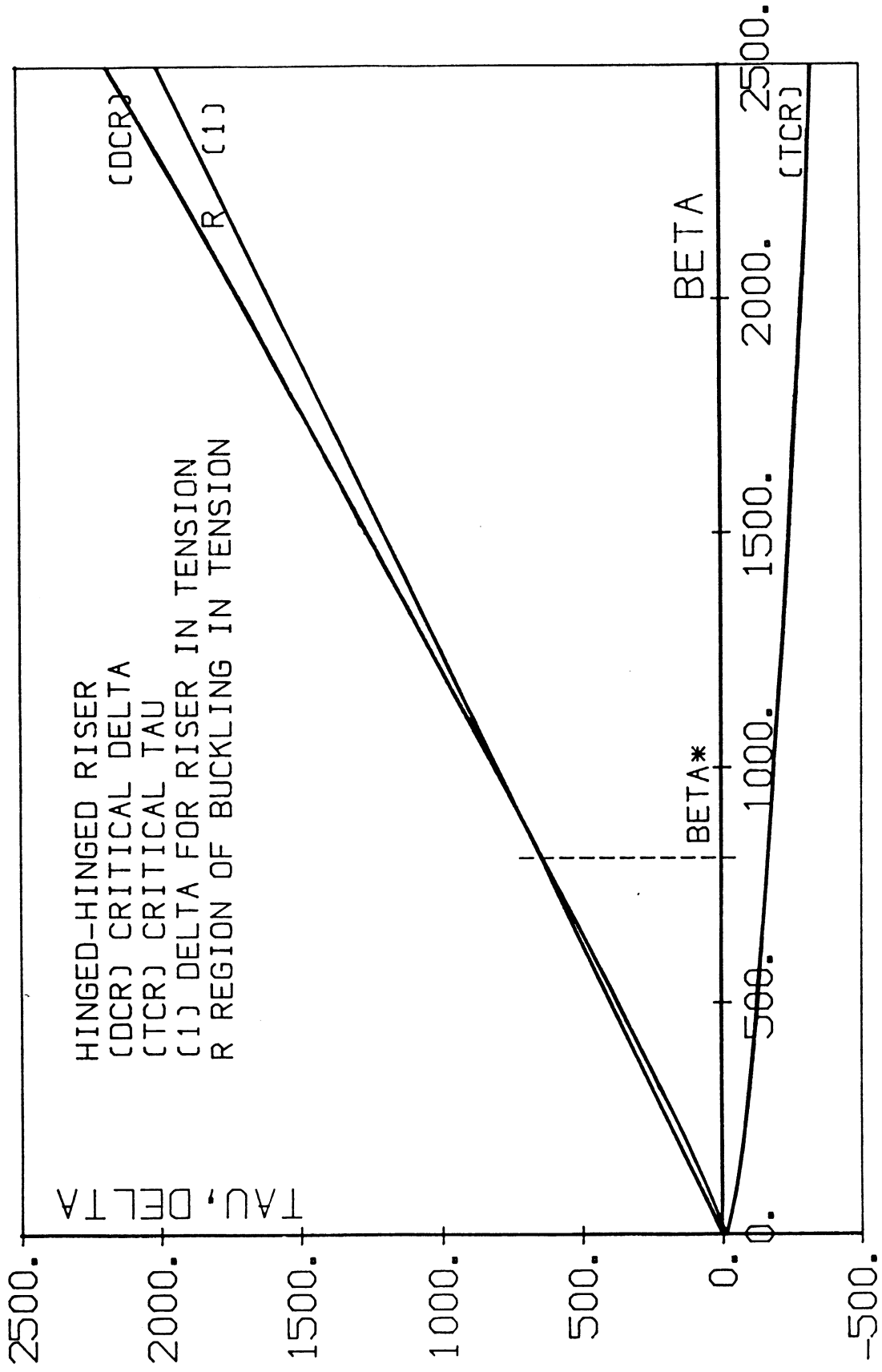

Figure 1. Stability Boundary and Region of Buckling in Tension for a Hinged-Hinged Riser

We define β^* (BETA*) as the abscissa of the intersection of lines [DCR] and [1] in Figure 1. This point indicates the beginning of the dimensionless region of buckling of risers in tension. Curve [DCR] is convex, monotonically increasing and starts below point ($\beta=0$, $\delta=0$). Curve [1] is a straight line through the origin with a positive slope for a partially buoyed riser. This is true for all boundary conditions considered in this paper. Consequently the two curves will either intersect at one point or not intersect at all. The necessary and sufficient condition for their intersection is that

$$\eta\beta < \tau_{crit} + \beta = \delta_{crit} \quad , \tag{II-15}$$

or

$$\beta(1-\eta) > -\tau_{crit} \tag{II-16}$$

Using regression analysis we can show that the variation of τ_{crit} with β, for high β values, is approximately geometric and has the form

$$\tau_{crit} = -c^2\beta^{2/3} \quad , \tag{II-17}$$

where c is a real constant depending on the boundary conditions. Actually for $\beta \to \infty$ the asymptotic behavior of the stability boundaries is geometric with exponent 2/3 [9]. Therefore

$$\delta_{crit} = \beta - c^2\beta^{2/3} \tag{II-18}$$

Combining equations (II-15) and (II-17) or (II-16) and (II-18) we get for high β values

$$\beta(1-\eta) > c^2\beta^{2/3} \quad , \tag{II-19}$$

or

$$\beta^{1/3}(1-\eta) > c^2 \quad . \tag{II-20}$$

Inequality (II-20) can be satisfied as long as

$$\eta < 1 \quad . \tag{II-21}$$

that is when

$$\frac{W_{st} - B_m}{W_{st} + W_m - B_w - B_m} < 1 \qquad \text{(II-22)}$$

or equivalently when

$$W_m > B_w \qquad \text{(II-23)}$$

This indicates that if the destabilizing effect from the drilling fluid is more significant than the stabilizing effect of the external hydrostatic pressure there will be a value of β beyond which the riser will buckle in tension.

The value of β^* is a function of η and the boundary conditions. Figure 7 shows the value of β^* for the first buckling mode of risers with non-movable boundaries. It should be noticed that theoretically the value of W_m may become high enough to cause buckling of risers in tension in higher modes.

II.2. Variation of TTR with the Riser Length

The phenomenon described in the previous section may occur for realistic operating conditions and even for relatively short risers. The following examples demonstrate the case. For a riser with

$$D_o = 0.506 \text{ m} \qquad \text{(II-24)}$$

$$D_i = 0.476 \text{ m} \qquad \text{(II-25)}$$

$$\rho_m = 1.5\, \rho_w \qquad \text{(II-26)} \quad , \quad B_m = .3\, B_w \qquad \text{(II-27)}$$

and

$$E = 30 \cdot 10^6 \text{ psi} = 2.07 \cdot 10^{11} \frac{Nt}{m^2} \qquad \text{(II-28)}$$

we can transform the stability boundary from the dimensionless form in Figures 1 and 2 to the dimensional one in Figures 3 and 4 respectively. Using equations (II-10) and (I-2). Similarly we can transform the first inequality of (II-14), that is lines [1] in Figures 1 and 2 to lines [1] in Figures 3 and 4 respectively.

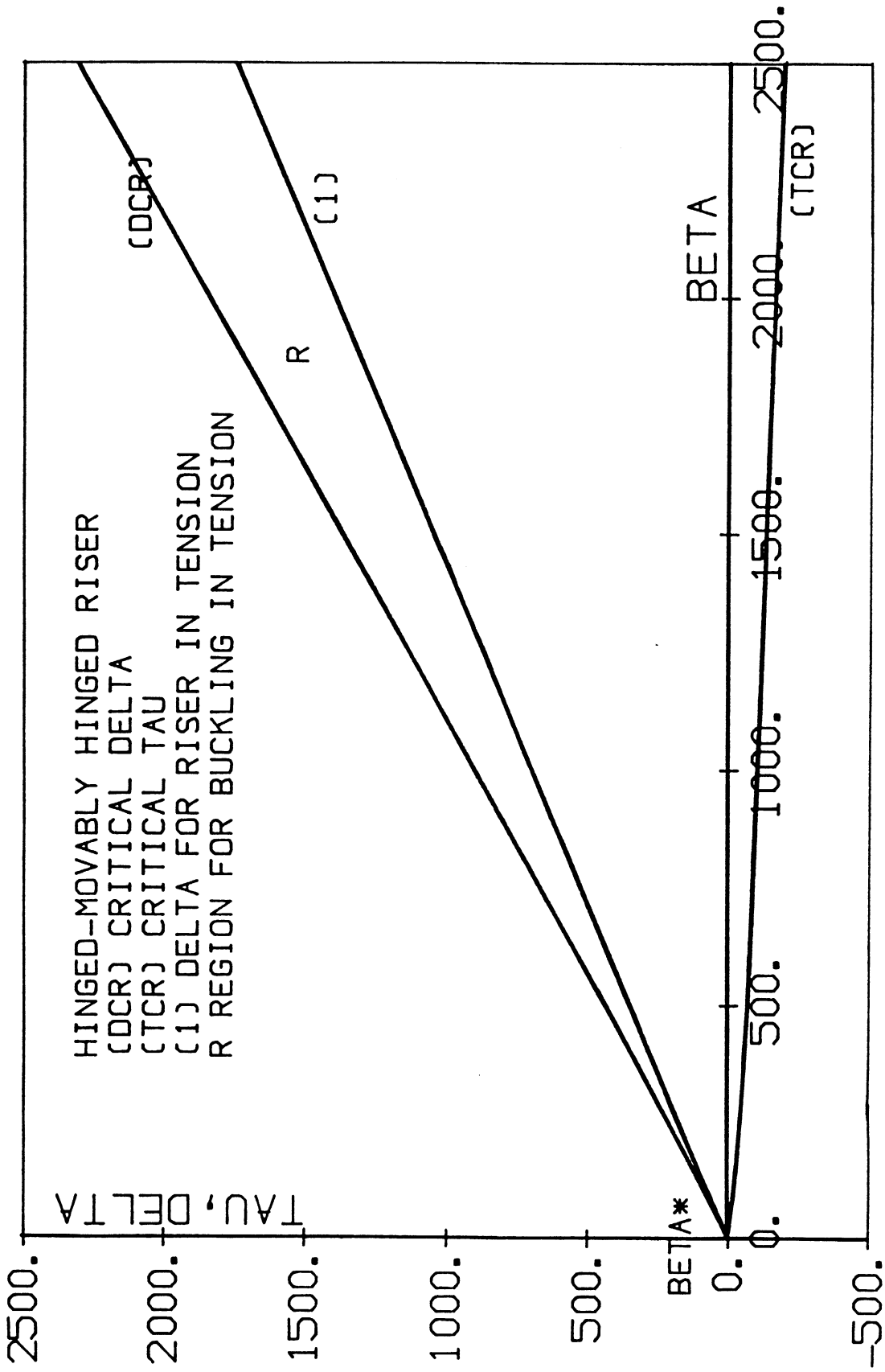

Figure 2. Stability Boundary and Region of Buckling in Tension for a Hinged-Movably Hinged Riser

Figure 3 shows, for this particular example, the region of buckling in tension for hinged-hinged risers. The intersection of lines [1] and [TTCR] occurs for relatively short risers. That is for

$$L \gtrsim 265 \text{ m} \qquad \text{(II-29)}$$

a hinged-hinged riser with the particulars shown in Figure 3 may buckle in tension.

Figure 4 is similar to Figure 3 for hinged-movably hinged risers. In this case buckling of risers in tension due to internal pressure may occur for

$$L \gtrsim 160\text{m} \qquad \text{(II-30)}$$

II.3. Distribution of Supporting Forces between TTR and B_m

For a 500 m riser with the same geometric particulars as the one in the previous example we can transform the dimensionless stability boundaries in Figures 1 and 2 to the dimensional ones in Figures 5 and 6 respectively.

Each riser is supported by top tension TTR and buoyancy modules measured by the ratio B_m/B_w . Figure 5 shows the stability boundary and the buckling in tension region for hinged-hinged risers in the TTR , B_m/B_w plane. Further Figure 5 shows the proper distribution of the riser supporting forces between top tension and buoyancy in order to prevent buckling.

In a similar manner we can transform Figure 2 to Figure 6 for a 500 m hinged-movably hinged riser with the same geometric particulars.

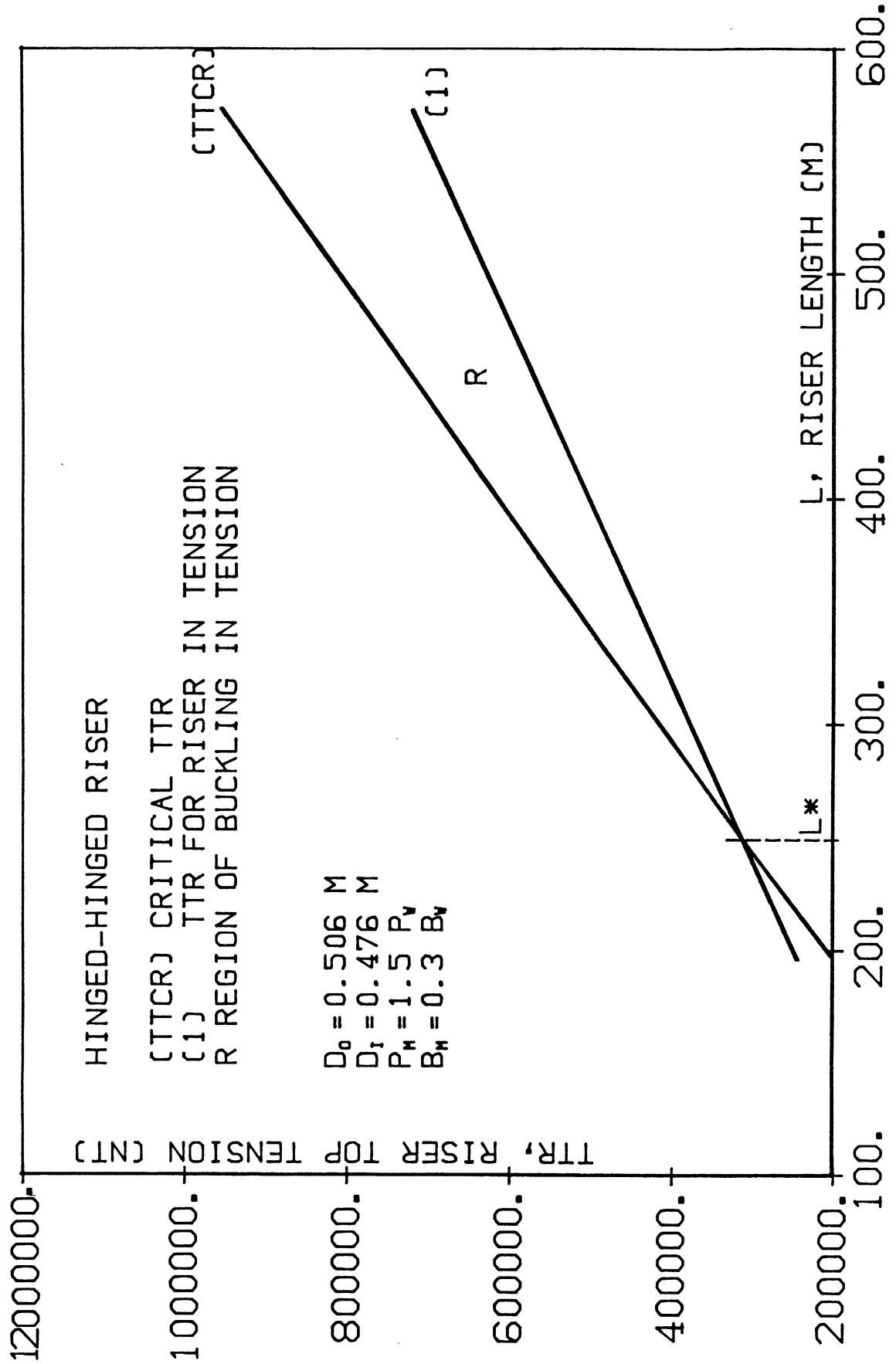

Figure 3. Top Tension versus Length for a Hinged-Hinged Riser

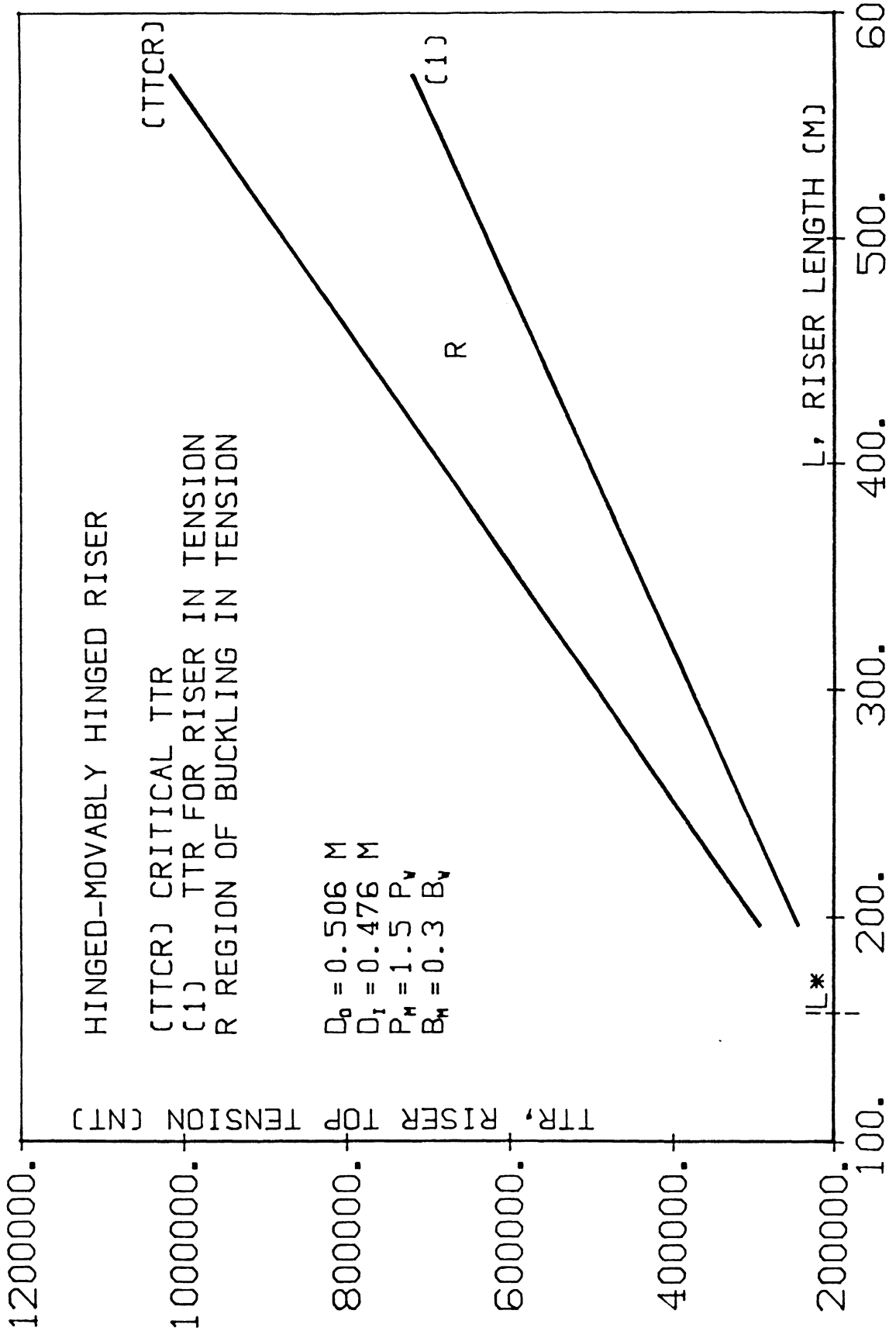

Figure 4. Top Tension versus Length for a Hinged-Movably Hinged Riser

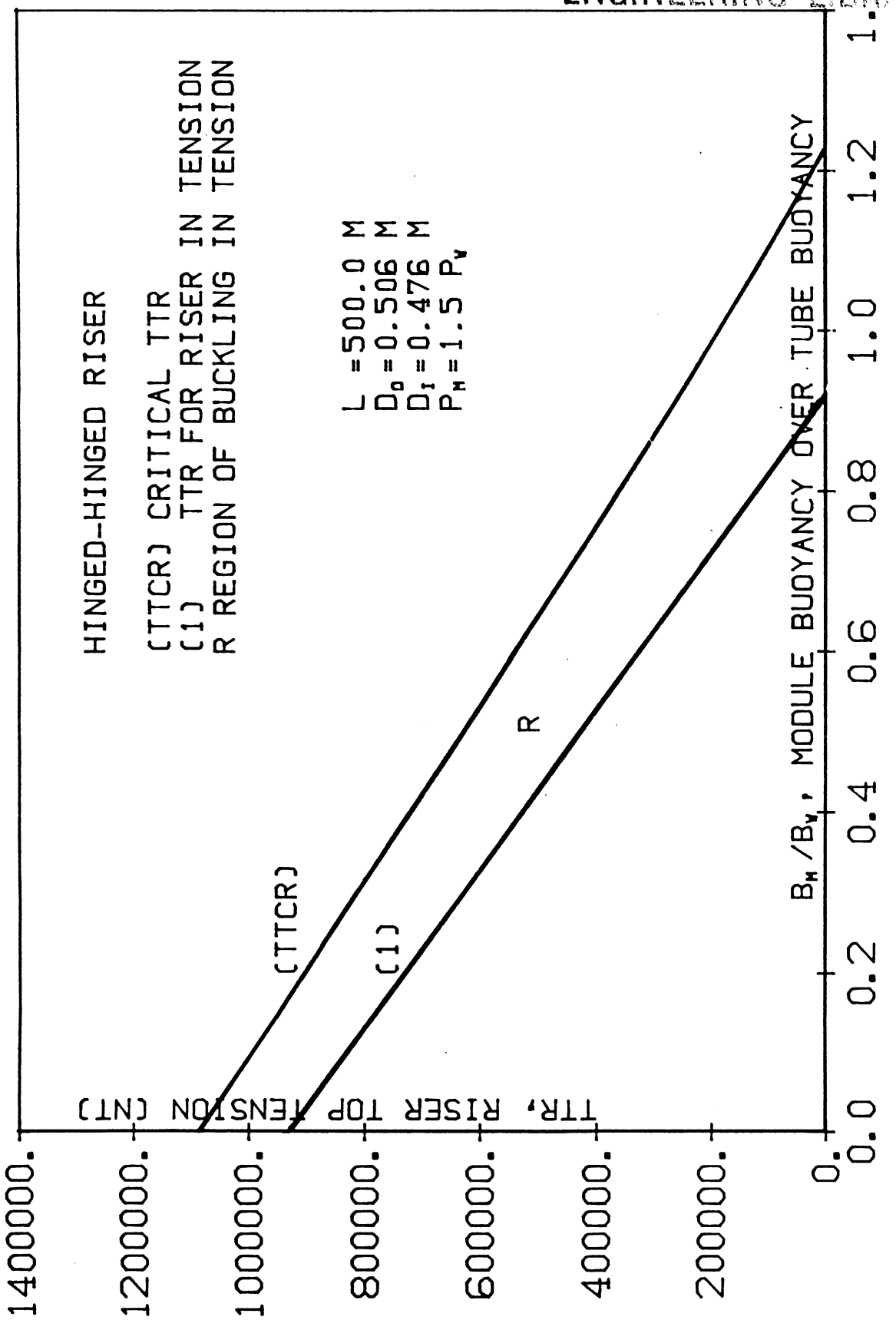

Figure 5. Distribution of Supporting Forces for a Hinged-Hinged Riser

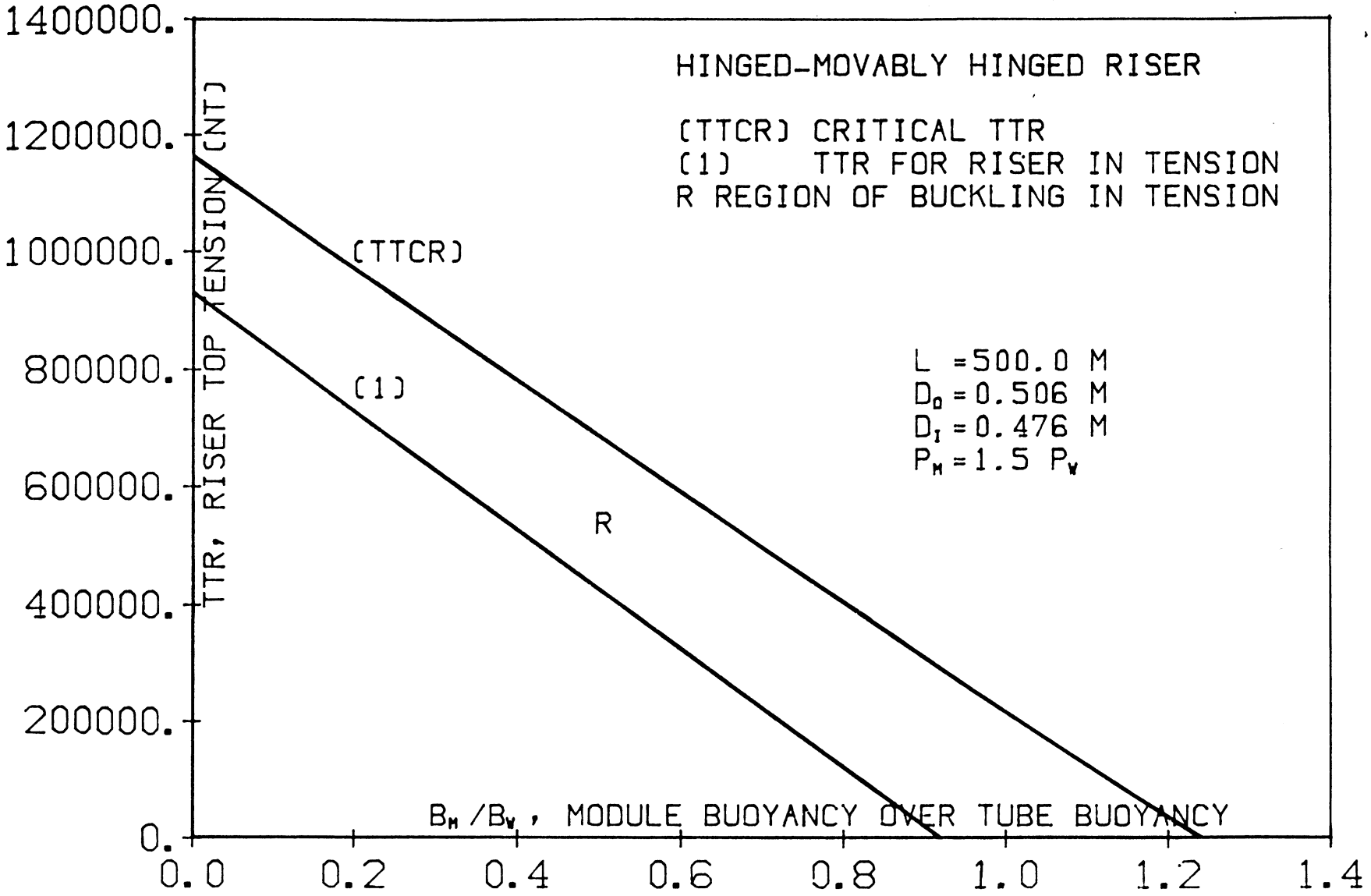

Figure 6. Distribution of Supporting Forces for a Hinged-Movably Hinged Riser

III. CRITICAL LENGTH FOR BUCKLING IN TENSION

An important dimensional quantity that can shed light into this counter-intuitive phenomenon is the critical length for which a riser, which is in tension along its entire length and has given geometric and loading particulars, may buckle globally as Euler column.

III.1. Definition of Critical Length

Using the definition of β^* from Chapter II and equation (I-2) we can define the critical length as

$$L^* = \sqrt[3]{\frac{\beta^* EI}{W_e}} \qquad \text{(III-1)}$$

Using equation (II-13) we can rewrite (III-1) as

$$L^* = \sqrt[3]{\frac{\beta^* EI}{W_{st-B_m}}} \sqrt[3]{\eta} \qquad \text{(III-2)}$$

β^* is a dimensionless quantity and, as shown in Chapter II, depends only on the boundary condition and η. Figure 7 depicts β^* versus η for the four boundary conditions for risers with nonmovable boundaries studied in this work. Similarly Figure 20 shows the dependence of β^* on η and the boundary conditions for risers with movable top support.

A better physical understanding of this phenomenon can be achieved by studying Figures 8 to 19 and 21 to 32 which show the critical length L^* versus dimensional quantities for a systematic variation of the riser geometric and loading particulars.

The systematic variation includes the following variations of variables and parameters.

1. Three different riser cross sections

$D_{o_1} = 0.25$ m (III-3) , $D_{i_1} = 0.23$ m (III-4)

$D_{o_2} = 0.55$ m (III-5) , $D_{i_2} = 0.515$ m (III-6)

$D_{o_3} = 1.05$ m (III-7) , $D_{i_3} = 0.95$ m (III-8)

2. Mud density varying in the range

$$1{,}200 \frac{kg}{m^3} \leq \rho_m \leq 2{,}250 \frac{kg}{m^3} \qquad \text{(III-9)}$$

3. Amount of buoyancy measured by the ratio B_m/B_w which takes four values 0.00, 0.20, 0.40, 0.60.

4. Finally in these figures the dependence of L^* on η is also shown. However, it should be emphasized that η and B_m/B_w are not independent variables and for all the numerical cases in the figures the value of the latter defines the former through equation (III-10)

$$\eta = \frac{W_{st}-B_m}{W_{st}+W_m-B_w-B_m} = \frac{W_{st}/B_w-B_m/B_w}{(W_{st}+W_m-B_w)/B_w-B_m/B_w} \qquad \text{(III-10)}$$

III.2. Critical Length for Hinged-Hinged Risers

For the three risers defined by equations (III-3) to (III-8) the value of the critical length is plotted in Figures 8, 9 and 10 versus the drilling mud density and for four different values of B_m/B_w . We can draw the following conclusions from these figures

1. The critical length decreases with increasing mud density. This was expected since it is the mud-static pressure inside the riser that reduces the effective riser tension and causes buckling.

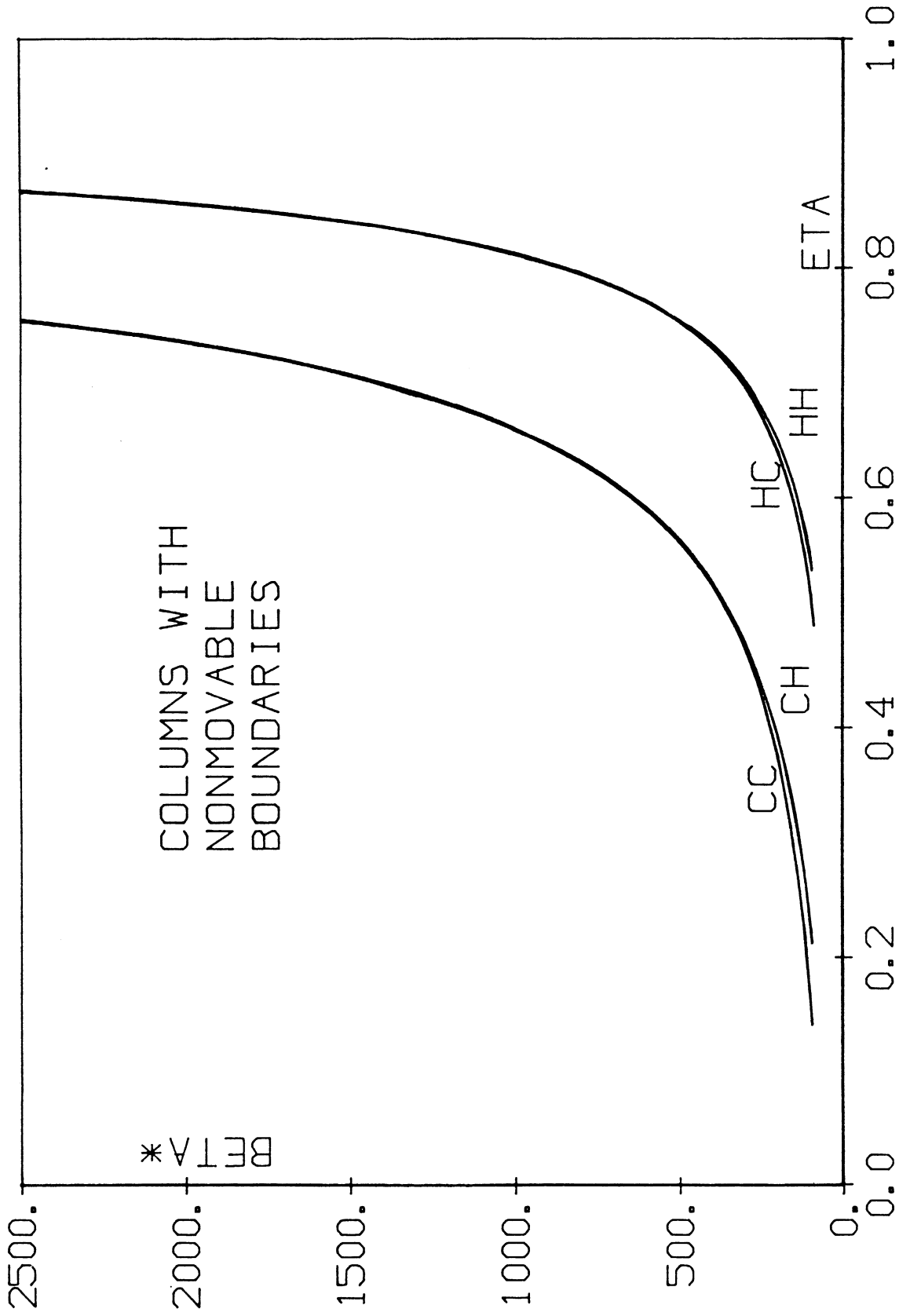

Figure 7. β^* versus η for Risers with Nonmovable Boundaries

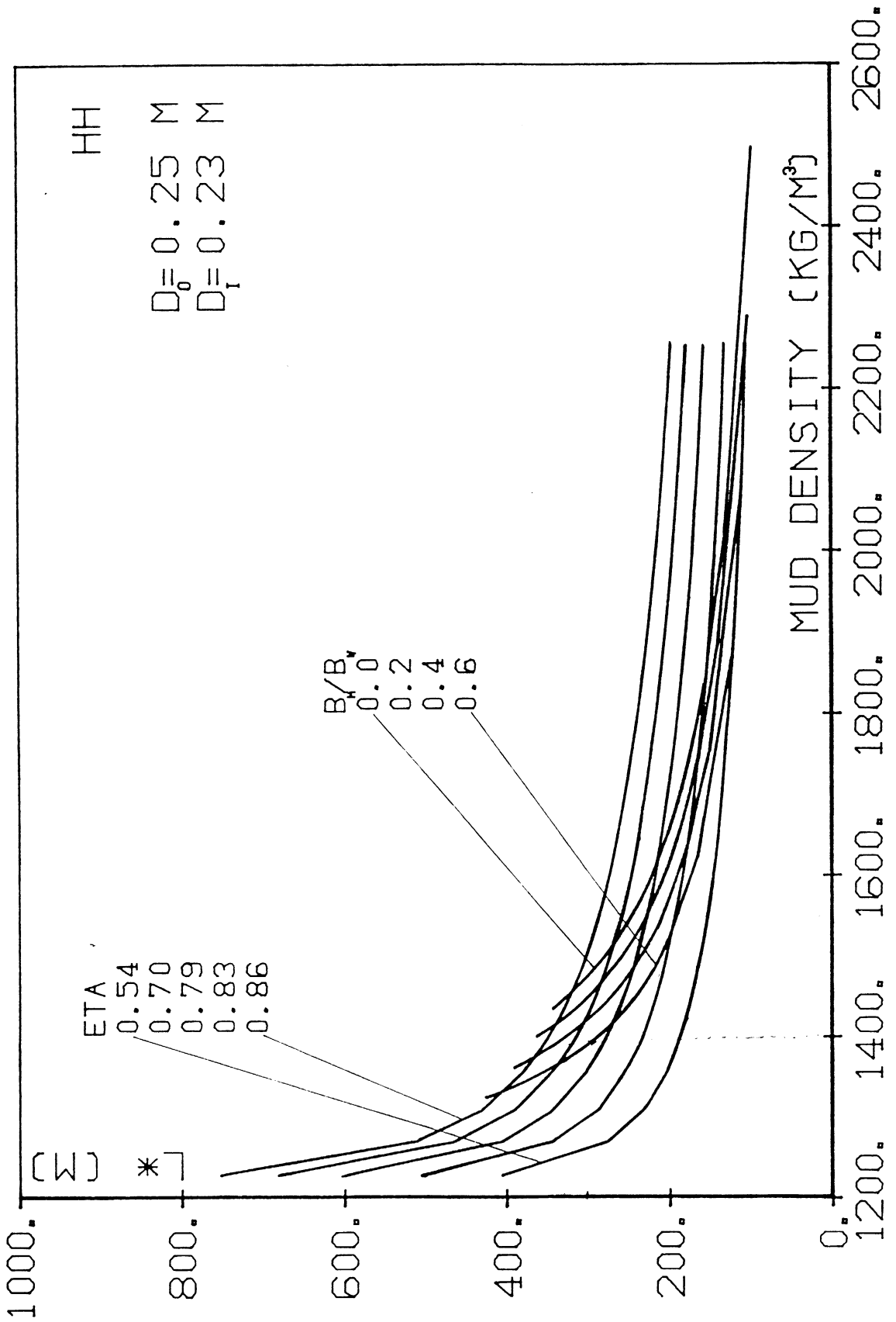

Figure 8. L* versus ρ_m for Hinged-Hinged Risers for D_O = 0.25m and D_I = 0.23m

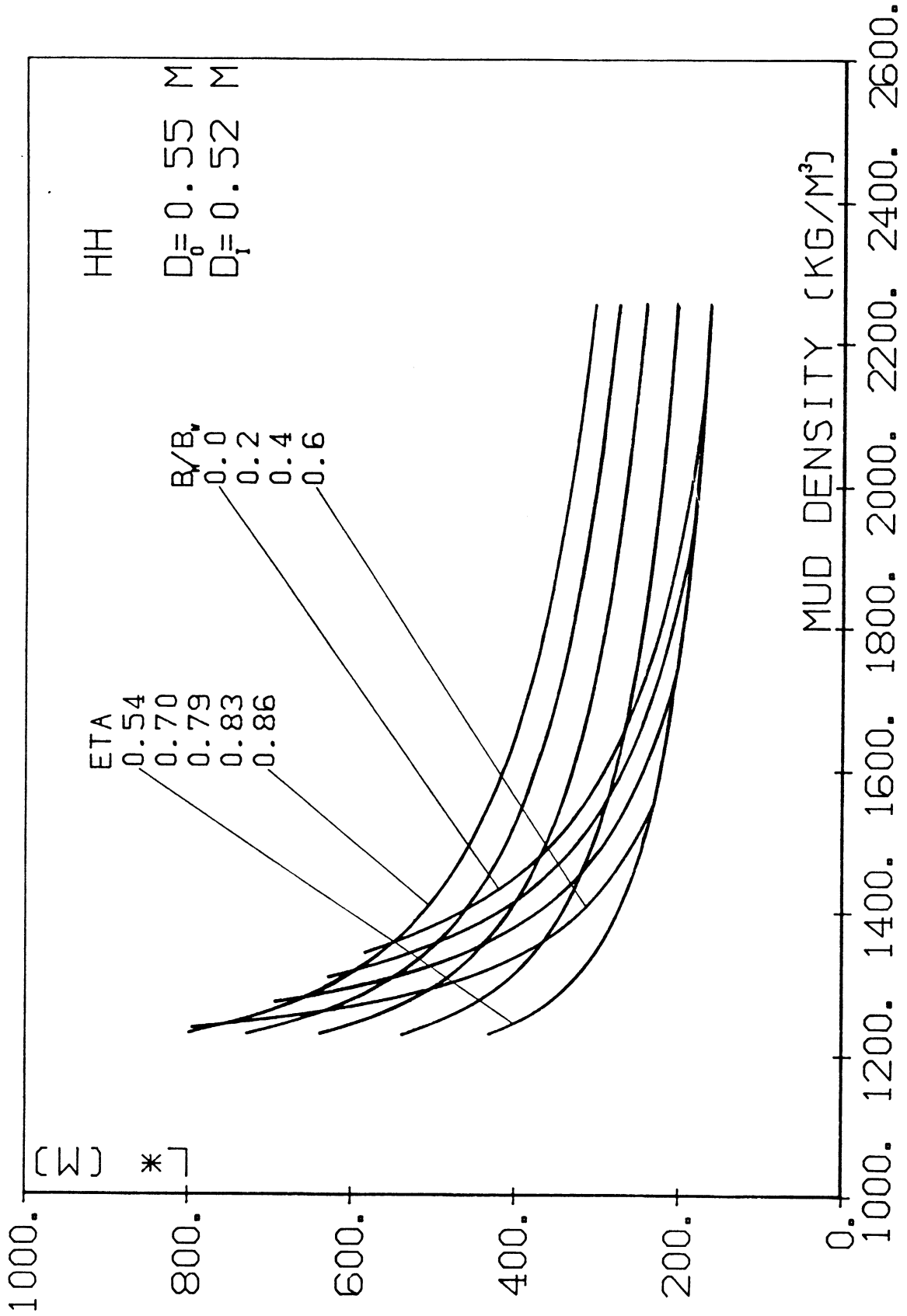

Figure 9. L* versus ρ_m for Hinged-Hinged Risers for D_o = 0.55m and D_i = 0.515m

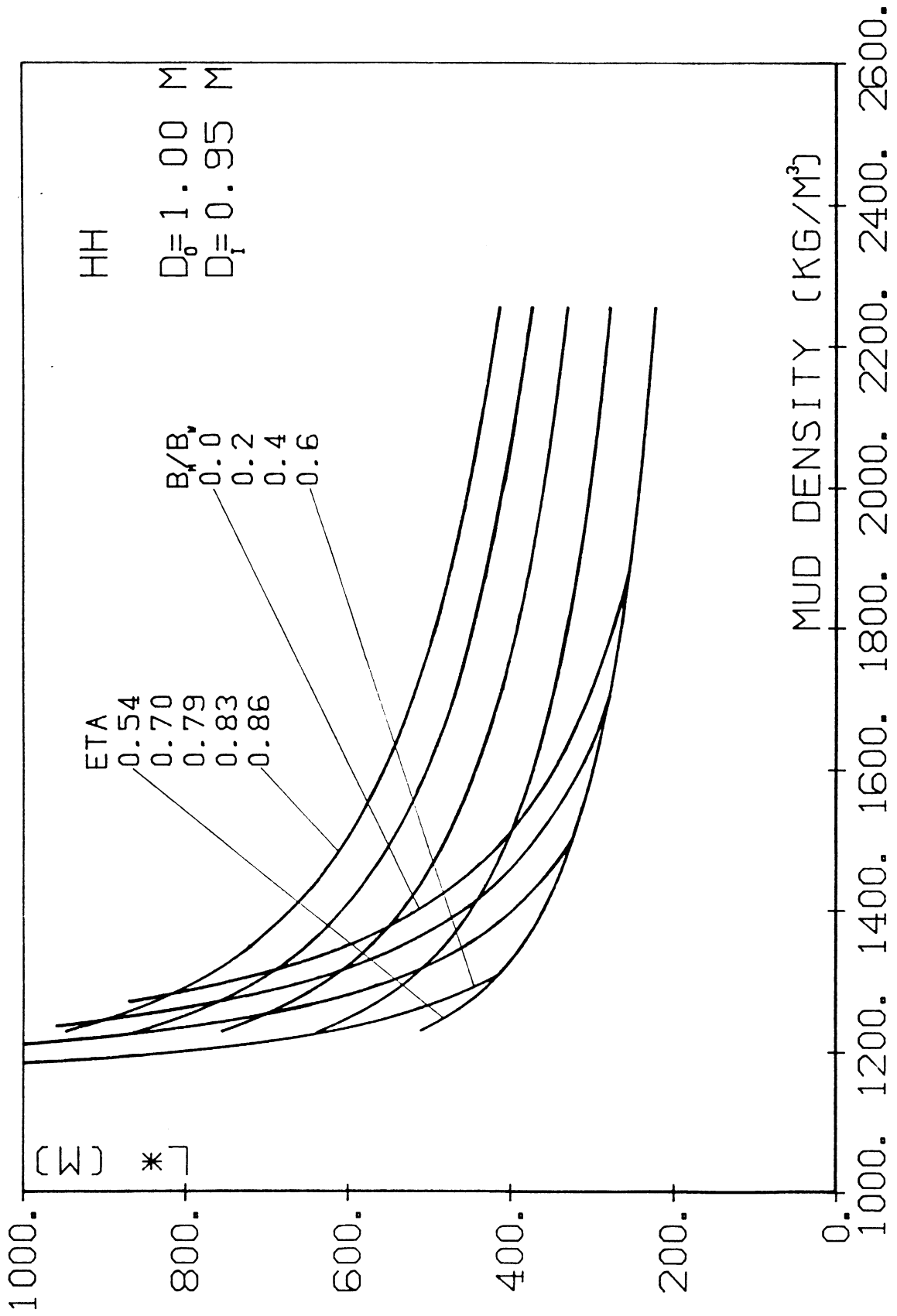

Figure 10. L* versus ρ_m for Hinged-Hinged Risers for D_o = 1.00m and D_i = 0.95m

2. As the mud density decreases tending to the water density the critical length tends to infinity since the internal pressure destabilizing effect is counterbalanced by the external hydrostatic pressure stabilizing effect.

3. The critical length L^* increases with η, that is the ratio of the apparent weight of the riser to the effective riser weight. It should be noted that the apparent weight is that of the riser in vacuum minus the net buoyancy of the modules only as indicated by equation (III-10).

4. L^* decreases with increasing buoyancy support. At first this appears to be counter-intuitive. However, it should be noticed that for a given riser as the buoyancy provided by the modules increases η decreases.

5. For a given value of B_m/B_w, L^* decreases with increasing mud density.

6. L^* decreases faster as the mud density increases for a given B_m/B_w than for a constant value of η. This can be explained by the same argument used in item 4 above.

7. The critical length L^* increases with increasing riser size for the three risers considered in Figures 8, 9 and 10. However, this conclusion cannot be generalized since no specific criterion, other than experience, was used to compute the internal riser diameter, D_i, for a given D_o.

III.3. Critical Length for Clamped-Hinged Risers

Figures 11, 12 and 13 present results similar to those in 8, 9 and 10 respectively for clamped-hinged risers. The same conclusions as those in Section III.2. can be drawn for this set of boundary conditions,

III.4. Critical Length for Hinged-Clamped Risers

Figures 14, 15 and 16 present the results of this analysis for hinged-clamped risers. Obviously the numerical answers are different but the general conclusions are the same.

III.5. Critical Length for Clamped-Clamped Risers

Figures 17, 18 and 19 show the results of this systematic analysis for clamped-hinged risers and show similar trends as all the other nonmovable boundary cases.

Finally by comparing all Figures 8 to 19 we can derive the following conclusions

1. For given mud density, ρ_m , η or B_m/B_w , and riser size, the critical length L* changes with the riser boundary conditions and increases with increasing restriction imposed by the boundary conditions that is, in the following order (a) hinged-hinged riser, (b) hinged-clamped riser, (c) clamped-hinged riser and (d) clamped-clamped riser (see also Chapter IV).

2. L* is of the order of a few hundred meters only, even for relatively low values of the drilling mud density.

3. Figures 8 to 19 indicate that even for high values of η, buckling in tension may occur for relatively low values of mud density and L^*. This indicates that the exact δ_{crit} values must be used to compute the minimum values of the tension required at the top of the riser.

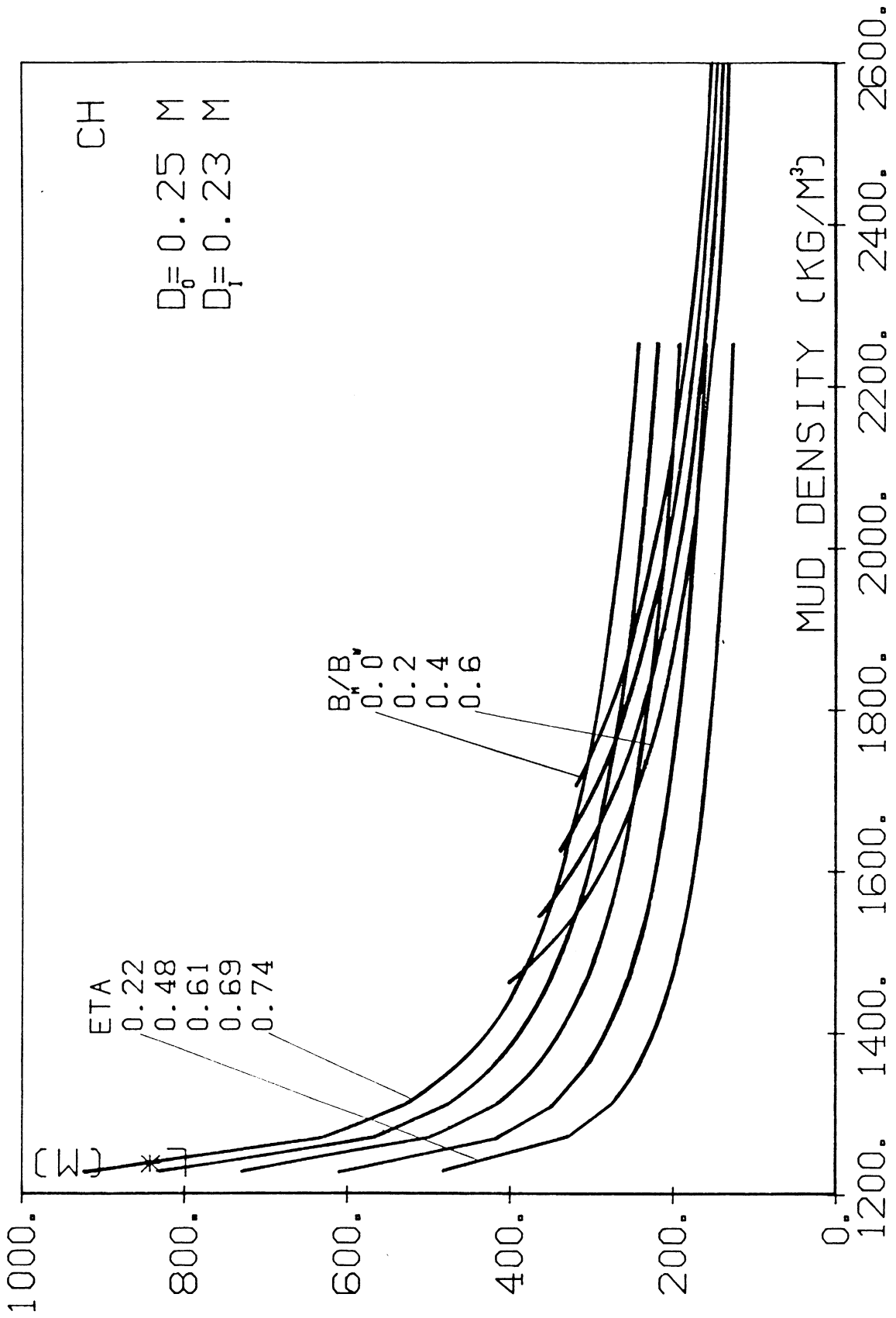

Figure 11. L* versus ρ_m for Clamped-Hinged Risers for D_o = 0.25m and D_i = 0.23m

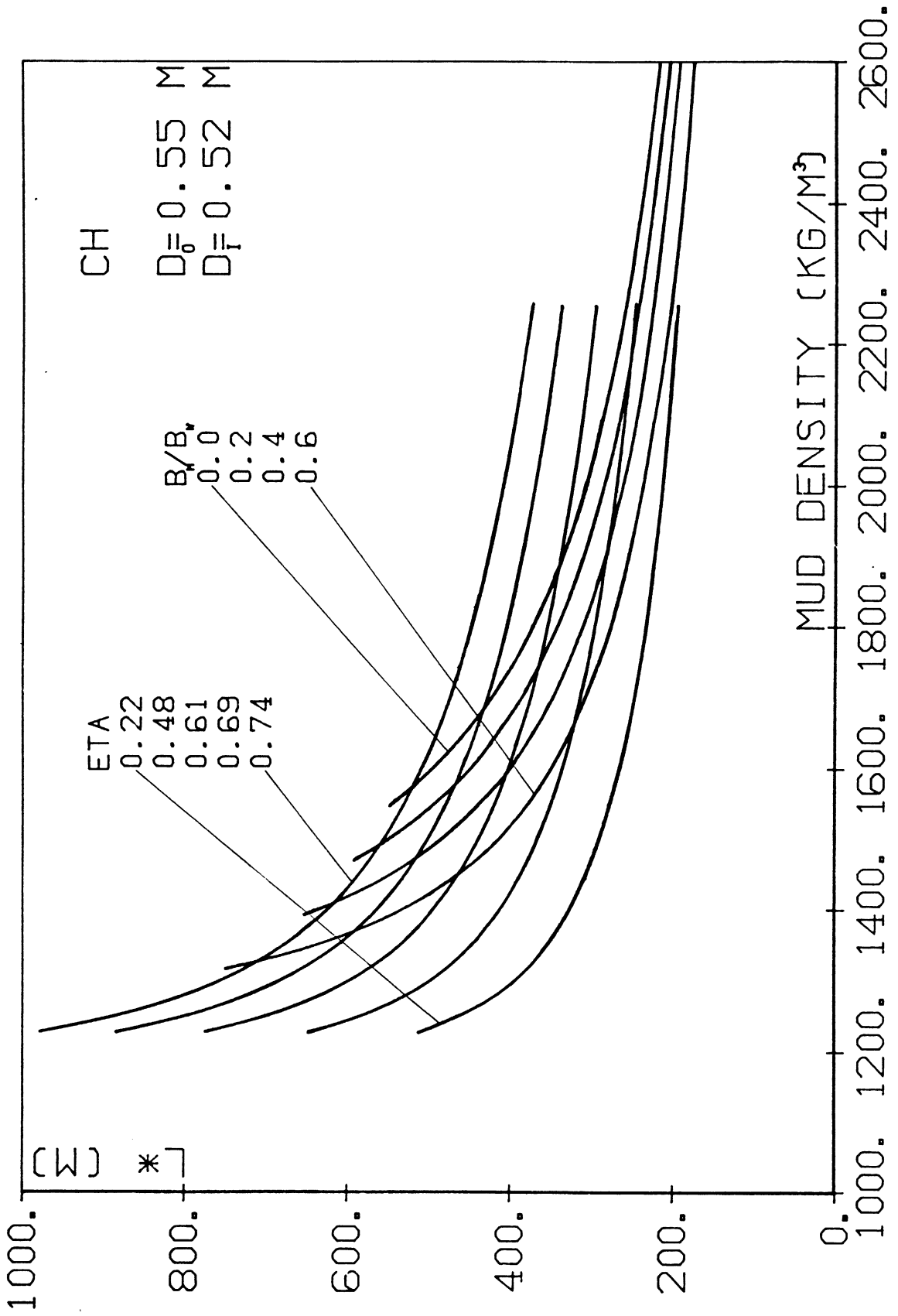

Figure 12. L^* versus ρ_m for Clamped-Hinged Risers for D_o = 0.55m and D_i = 0.515m

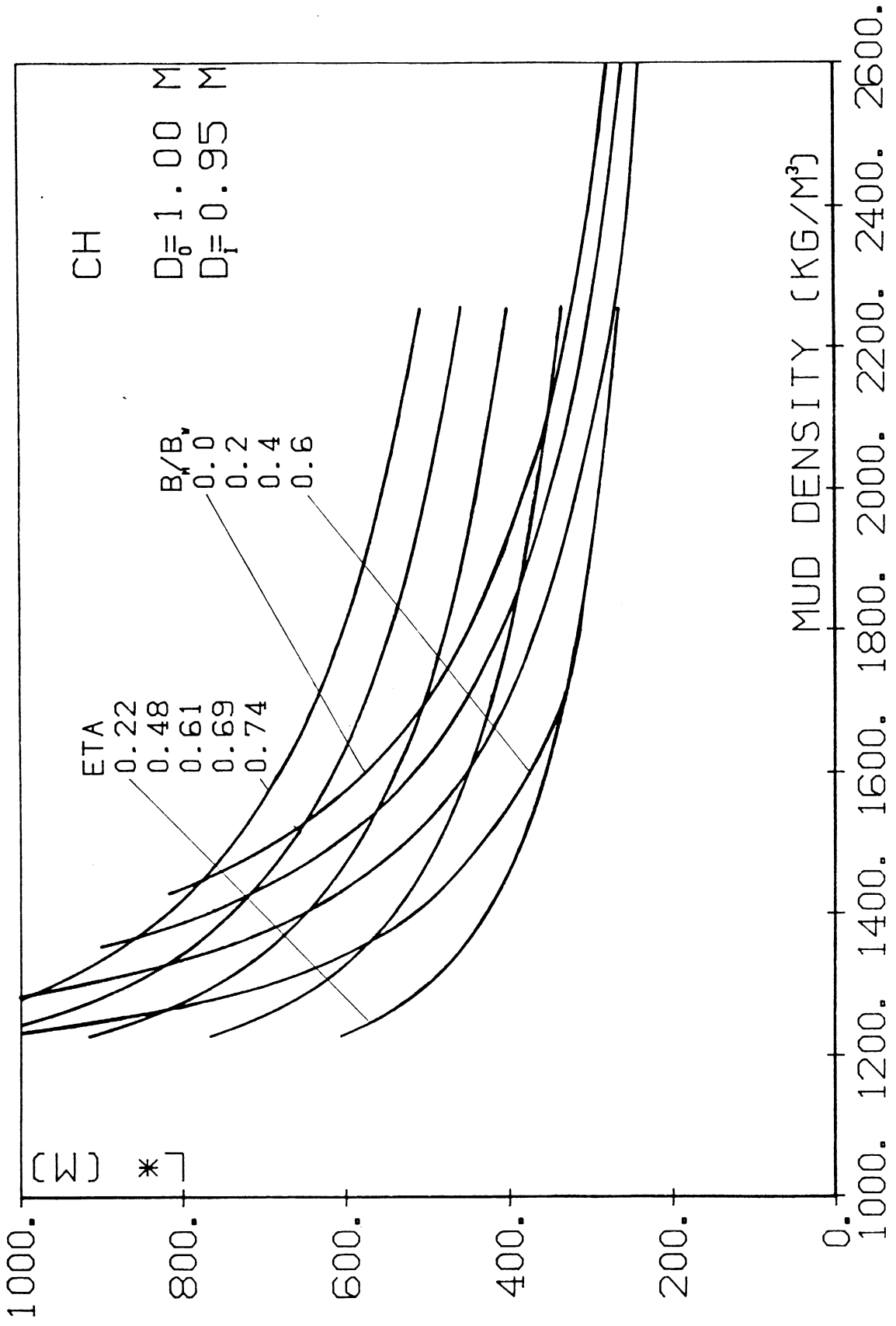

Figure 13. L* versus ρ_m for Clamped-Hinged Risers for D_o = 1.00m and D_i = 0.95m

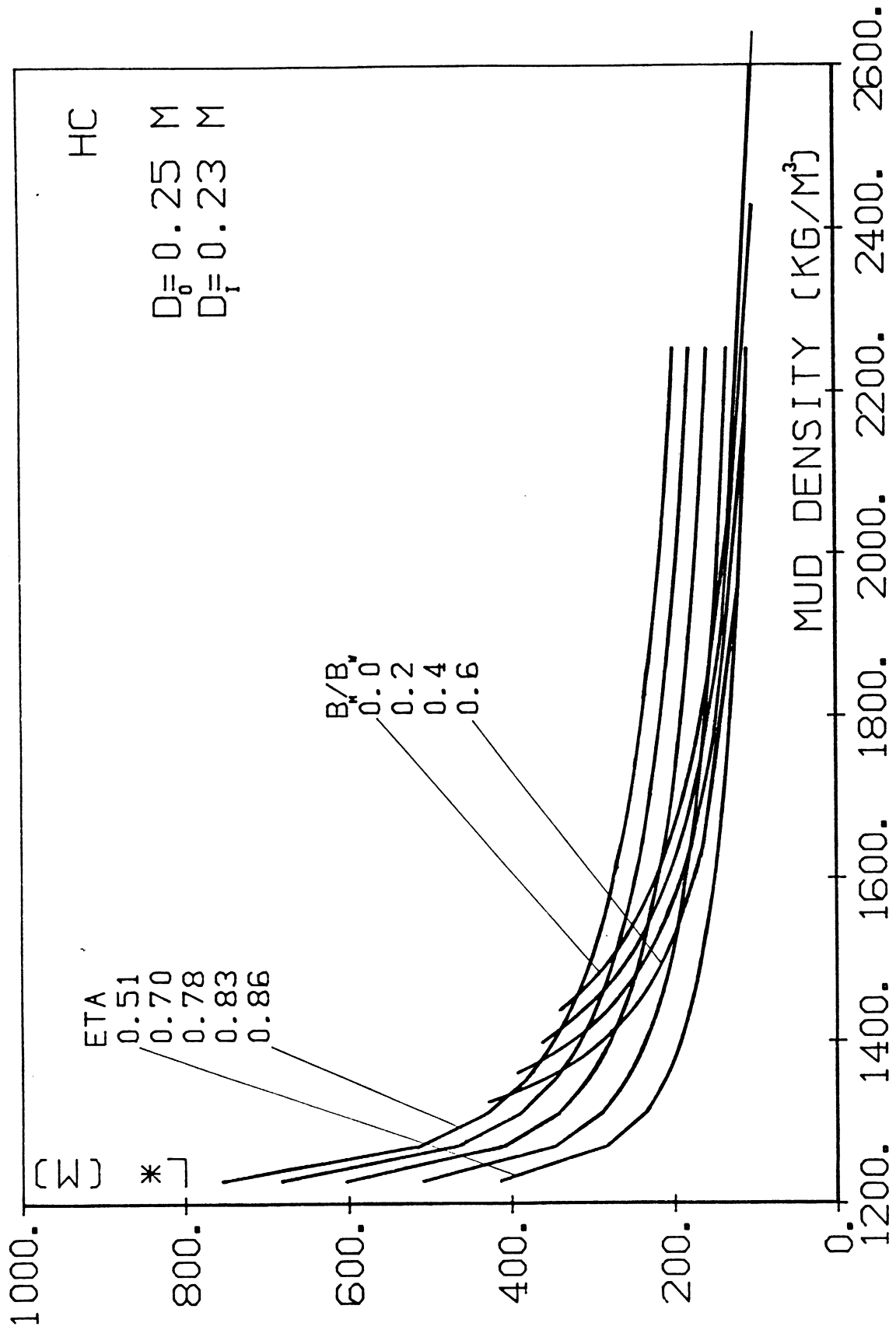

Figure 14. L* versus ρ_m for Hinged-Clamped Risers for D_o = 0.25m and D_i = 0.23m

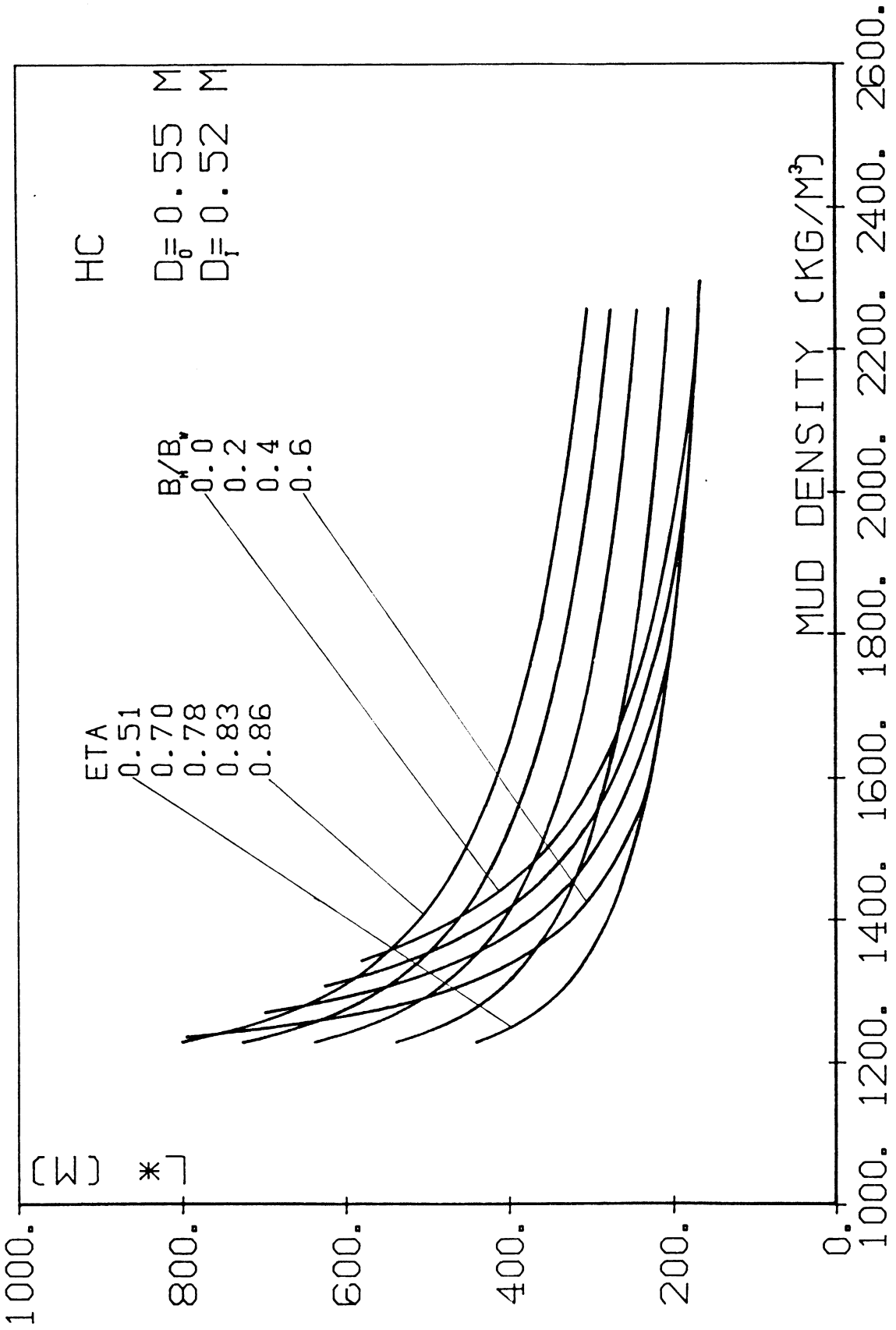

Figure 15. L* versus ρ_m for Hinged-Clamped Risers for D_O = 0.55m and D_i = 0.515m

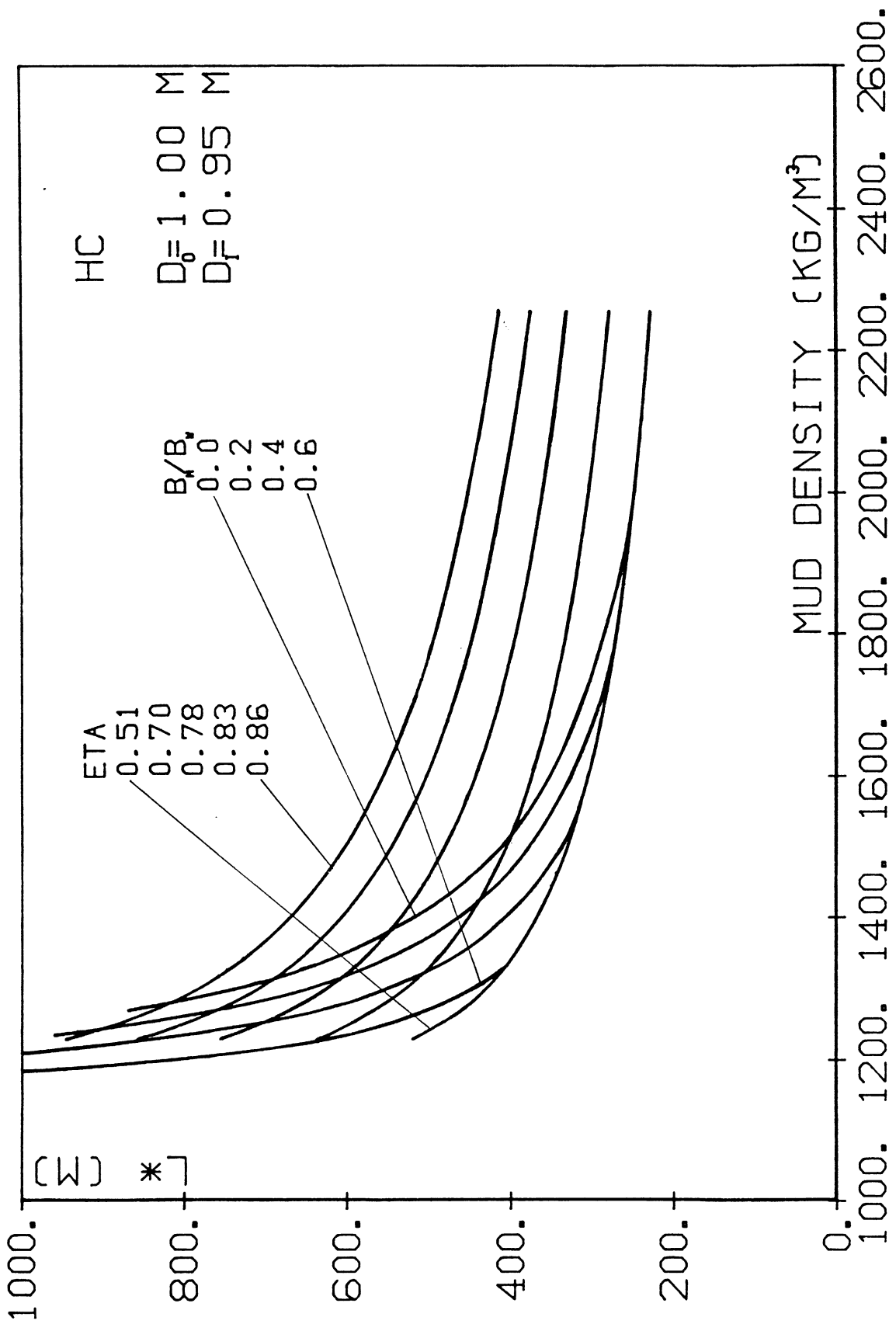

Figure 16. L_* versus ρ_m for Hinged-Clamped Risers for D_o = 1.00m and D_i = 0.95m

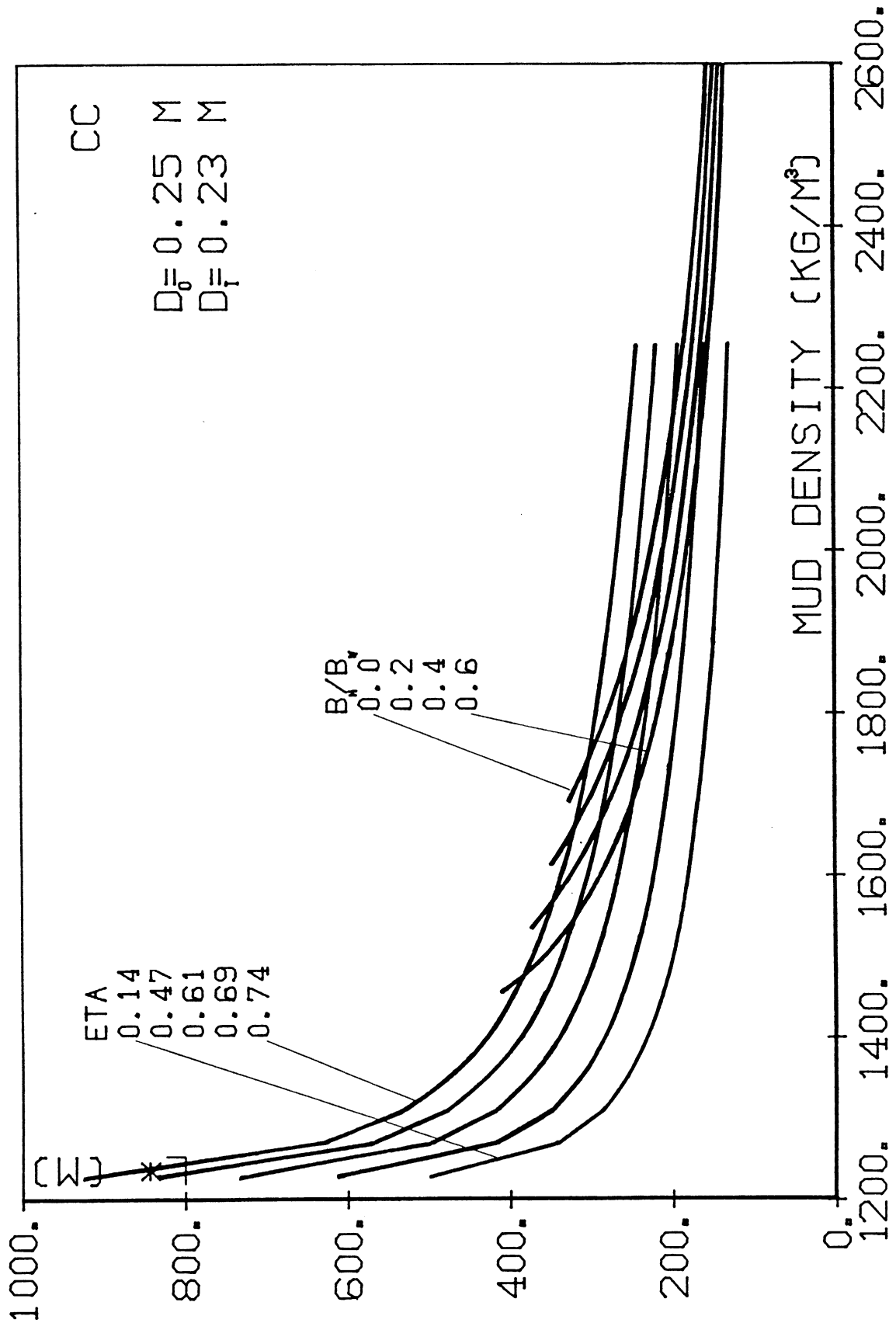

Figure 17. L* versus ρ_m for Clamped-Clamped Risers for D_o = 0.25m and D_i = 0.23m

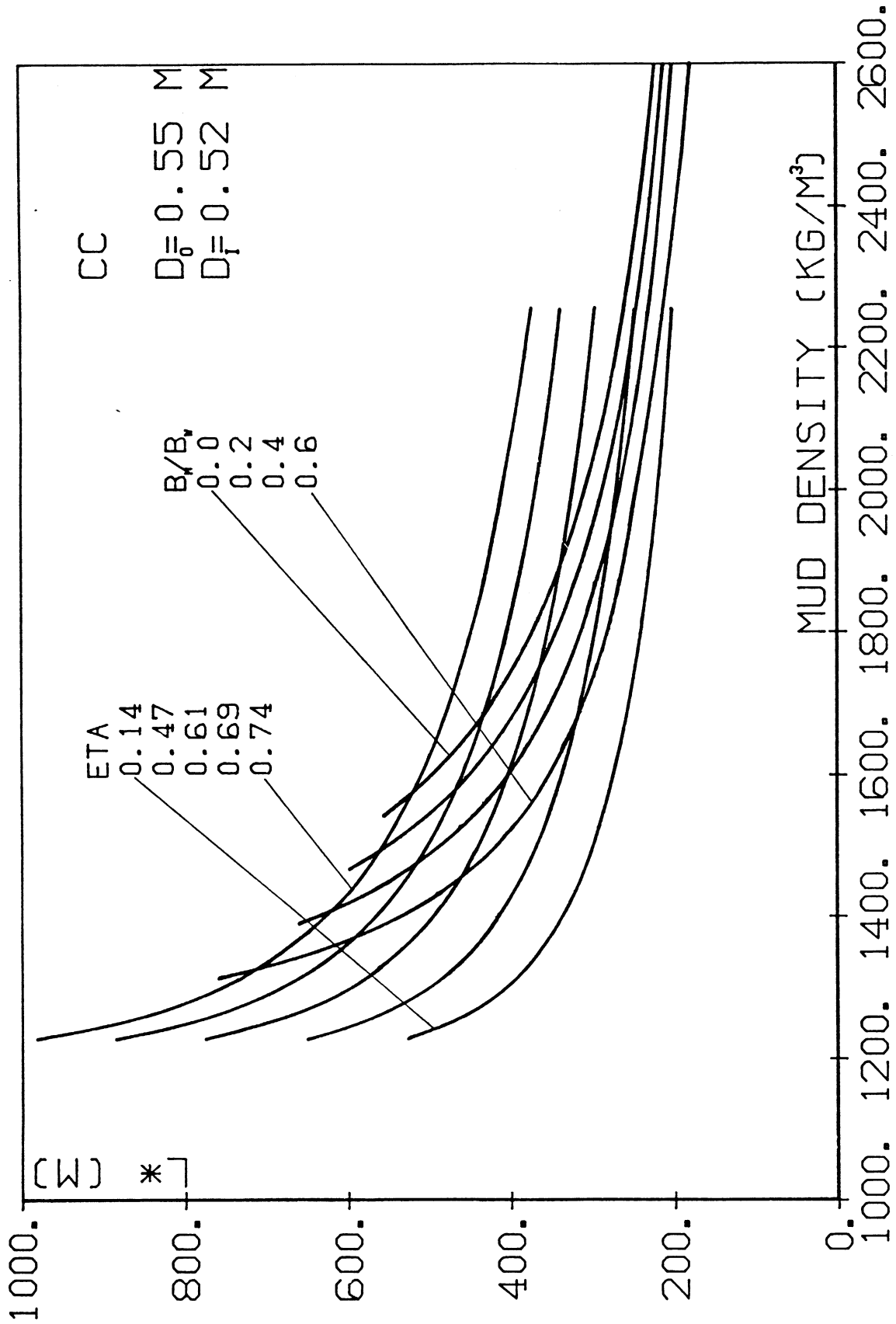

Figure 18. L* versus ρ_m for Clamped-Clamped Risers for D_o = 0.55m and D_i = 0.515m

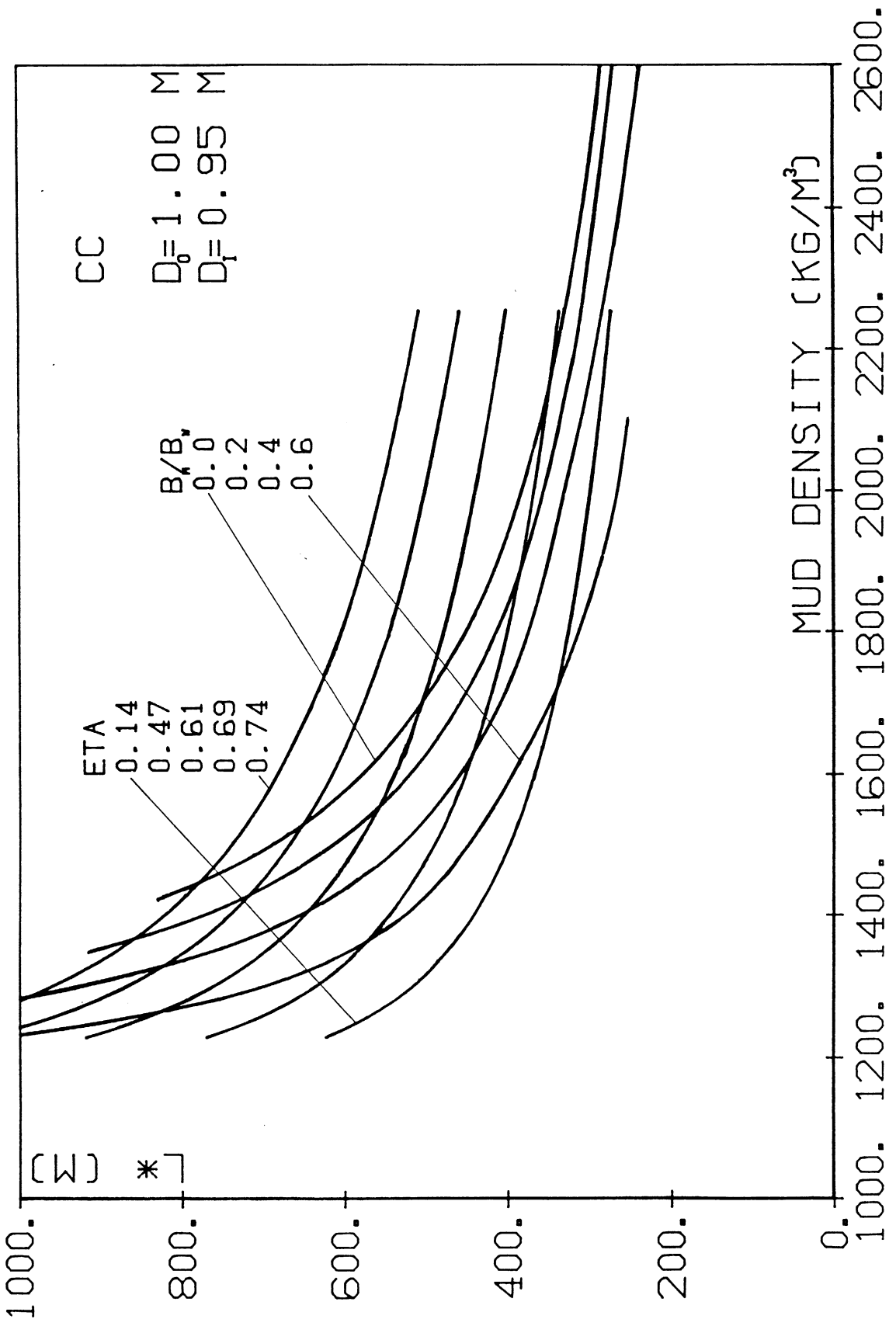

Figure 19. L* versus ρ_m for Clamped-Clamped Risers for D_o = 1.00m and D_i = 0.95m

III.6. Critical Length for Hinged-Movably Hinged Risers

For this set of boundary conditions, Figures 21, 22 and 23 show L^* versus ρ_m for the same systematic variation of parameters as the one for risers with nonmovable boundaries. The conclusions listed in Section III.2. hold in this case and all the following cases of risers with movable boundaries.

III.7. Critical Length for Clamped-Movably Hinged Risers

Figures 24, 25 and 26 depict similar numerical results for the critical length of clamped-movably hinged risers.

III.8. Critical Length for Hinged-Movably Clamped Risers

The results for this set of boundary conditions are presented in Figures 27, 28, 29 and show the same type of dependence of L^* on ρ_m, B_m/B_w and riser size.

III.9. Critical Length for Clamped-Movably Clamped Risers

For this last set of boundary conditions the results are presented in Figures 30, 31 and 32. Comparing all four cases of risers with movable top support we can draw the following conclusions

1. For given ρ_m, η or B_m/B_w, and riser size the critical length L^* changes with the riser boundary conditions and increases with increasing restriction imposed by the boundary conditions, that is in the following order (a) hinged-movably hinged riser, (b) hinged-movably clamped riser, (c) clamped-movably hinged riser and (d) clamped-movably clamped riser (see also Chapter V).

2. L^* is of the order of a few hundred meters only, even for relatively low values of the drilling mud density.

3. Figures 21 to 32 show that even for high η values, buckling in tension may occur for relatively low values of ρ_m and L^* .

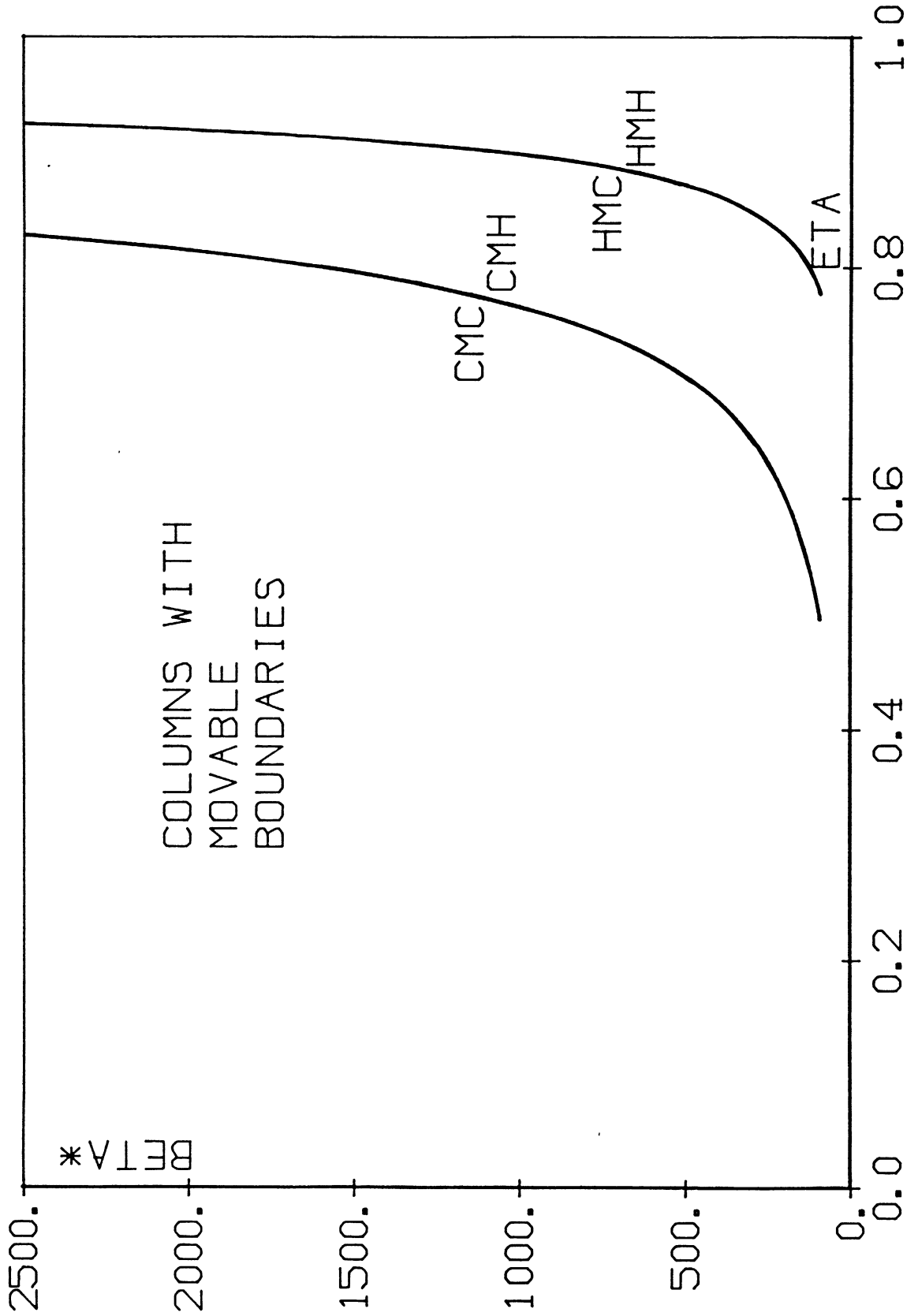

Figure 20. β^* versus η for Risers with Movable Boundaries

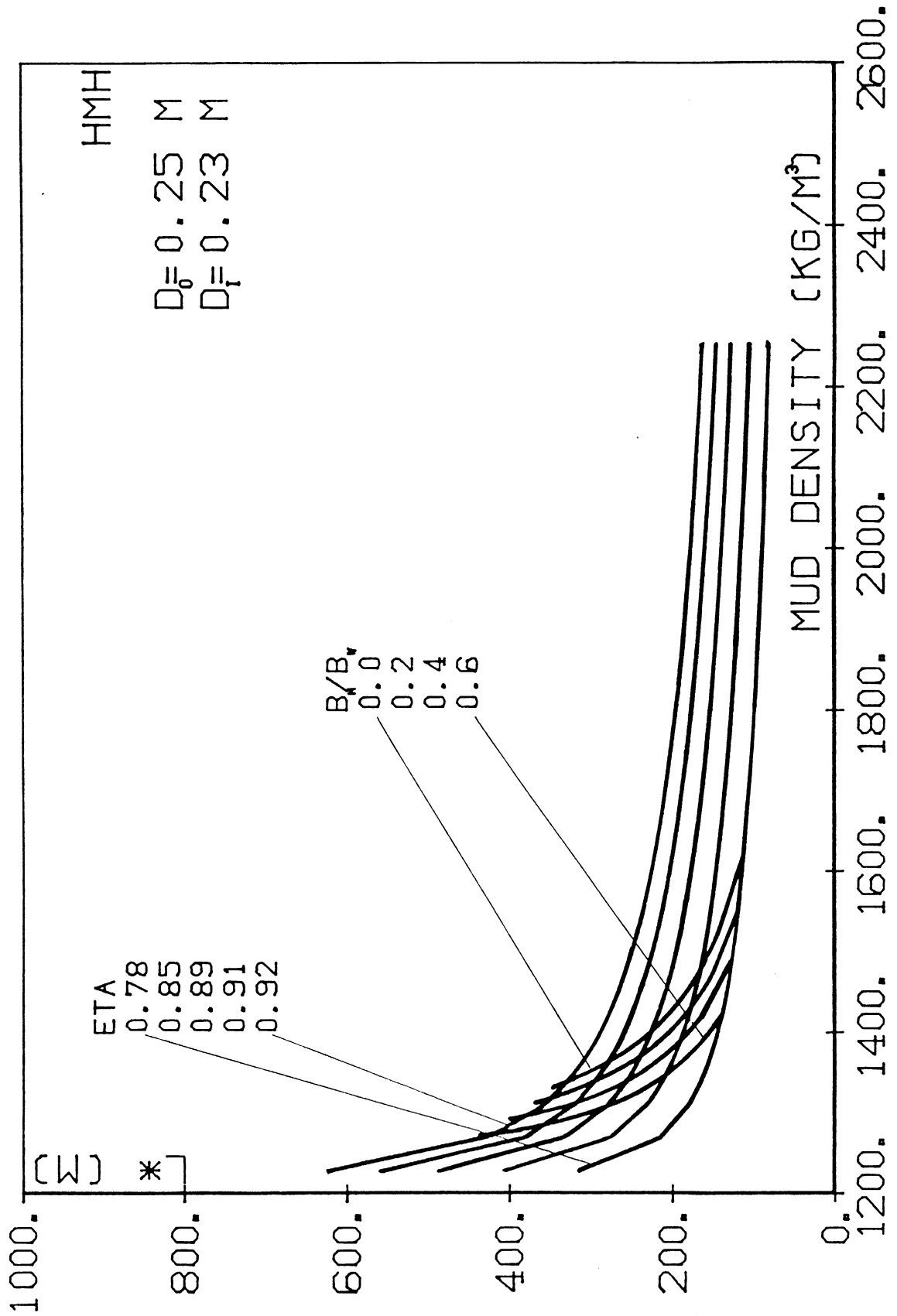

Figure 21. L* versus ρ_m for Hinged-Movably Hinged Risers for D_O = 0.25m and D_i = 0.23m

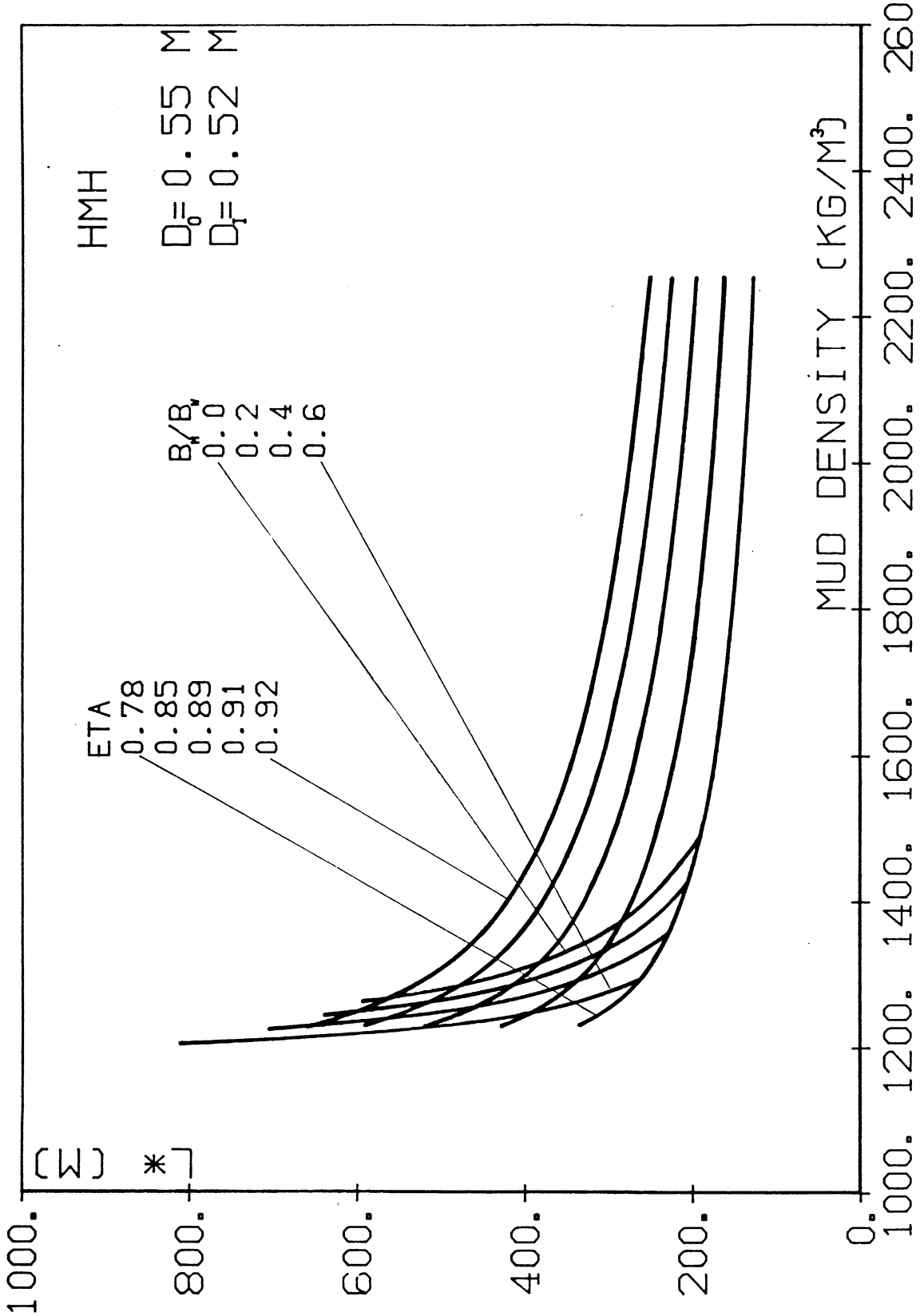

Figure 22. L* versus ρ_m for Hinged-Movably Hinged Risers for D_o = 0.55m and D_i = 0.515m

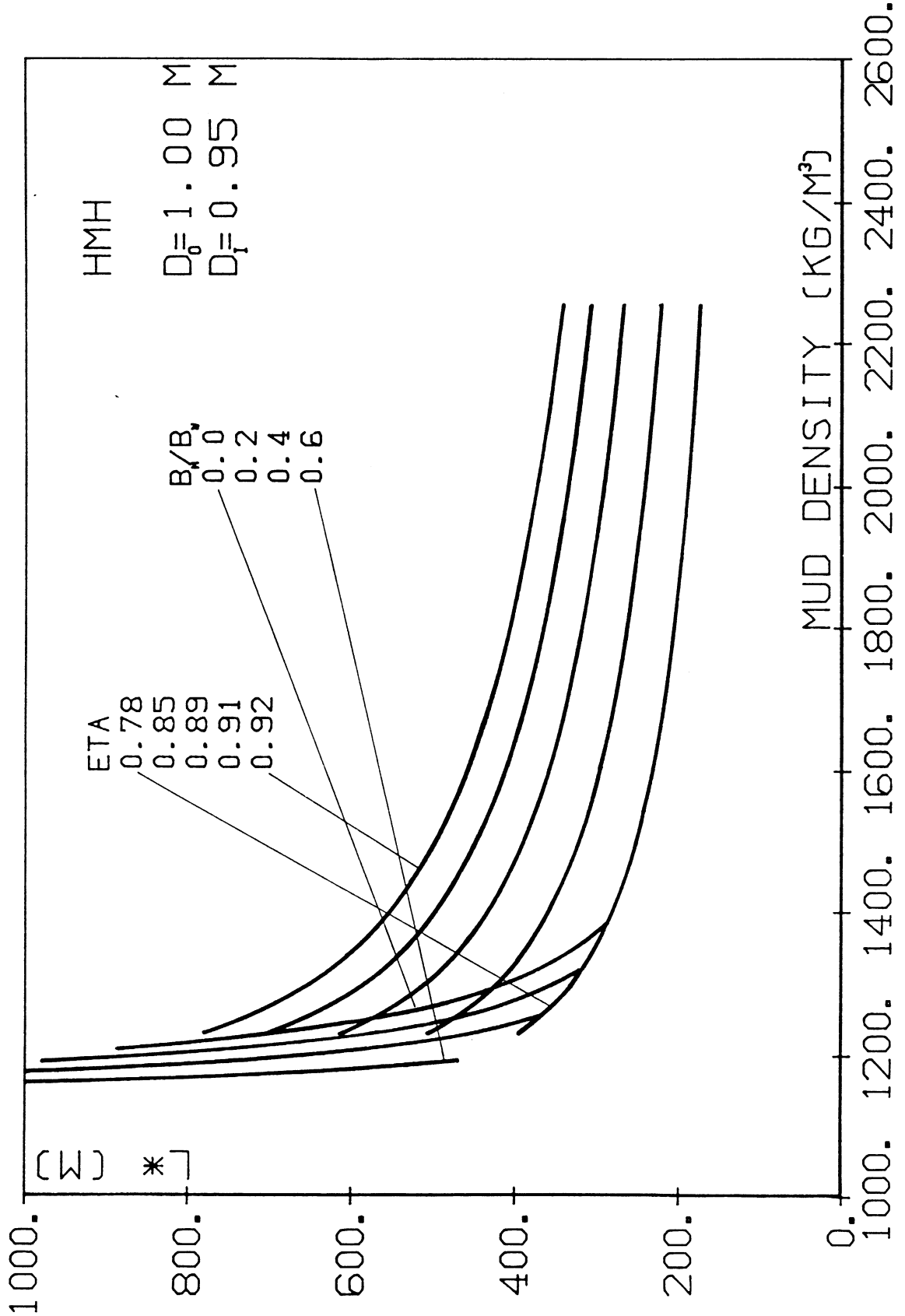

Figure 23. L* versus ρ_m for Hinged-Movably Hinged Risers for D_o = 1.00m and D_i = 0.95m

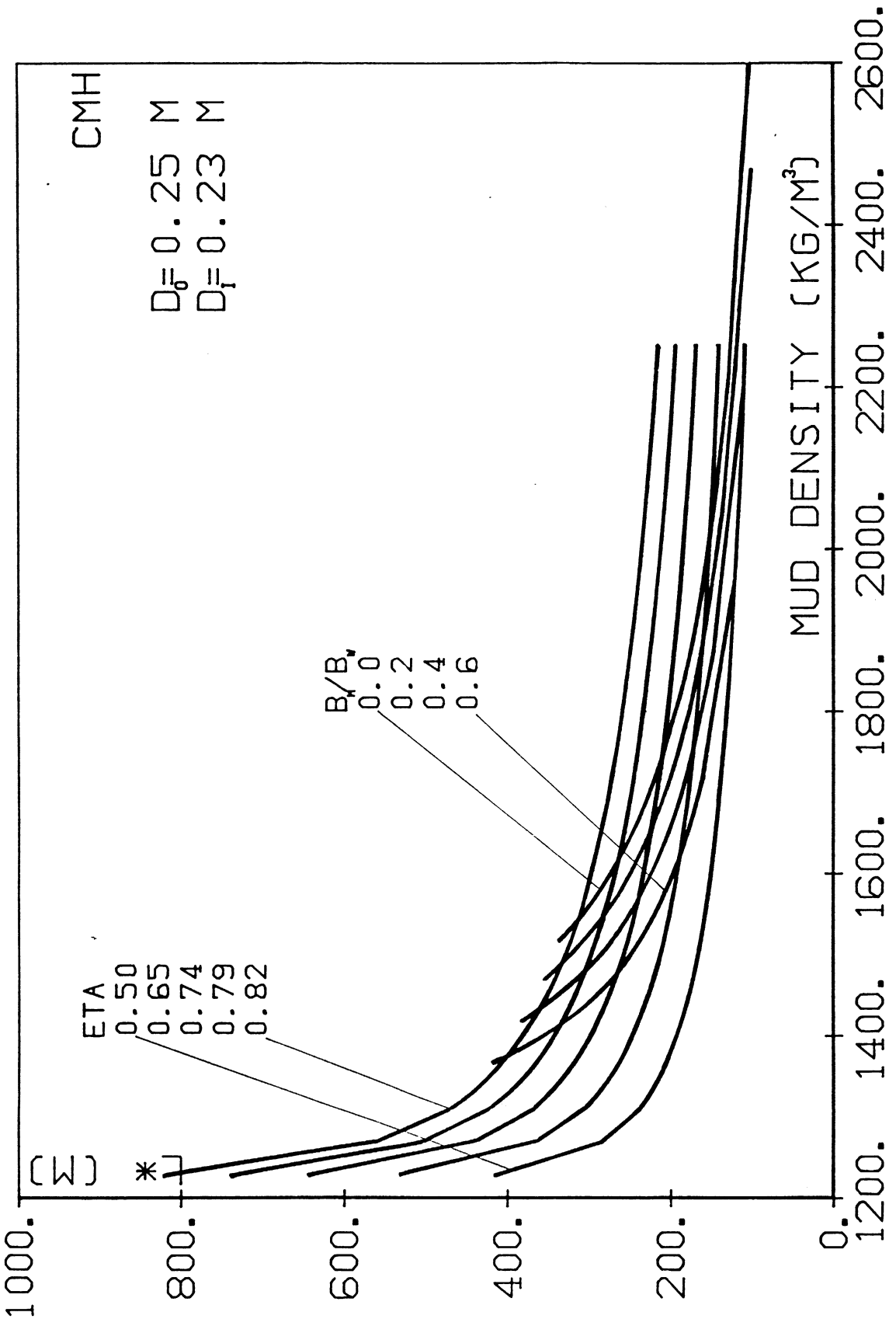

Figure 24. L* versus ρ_m for Clamped-Movably Hinged Risers for D_o = 0.25m and D_i = 0.23m

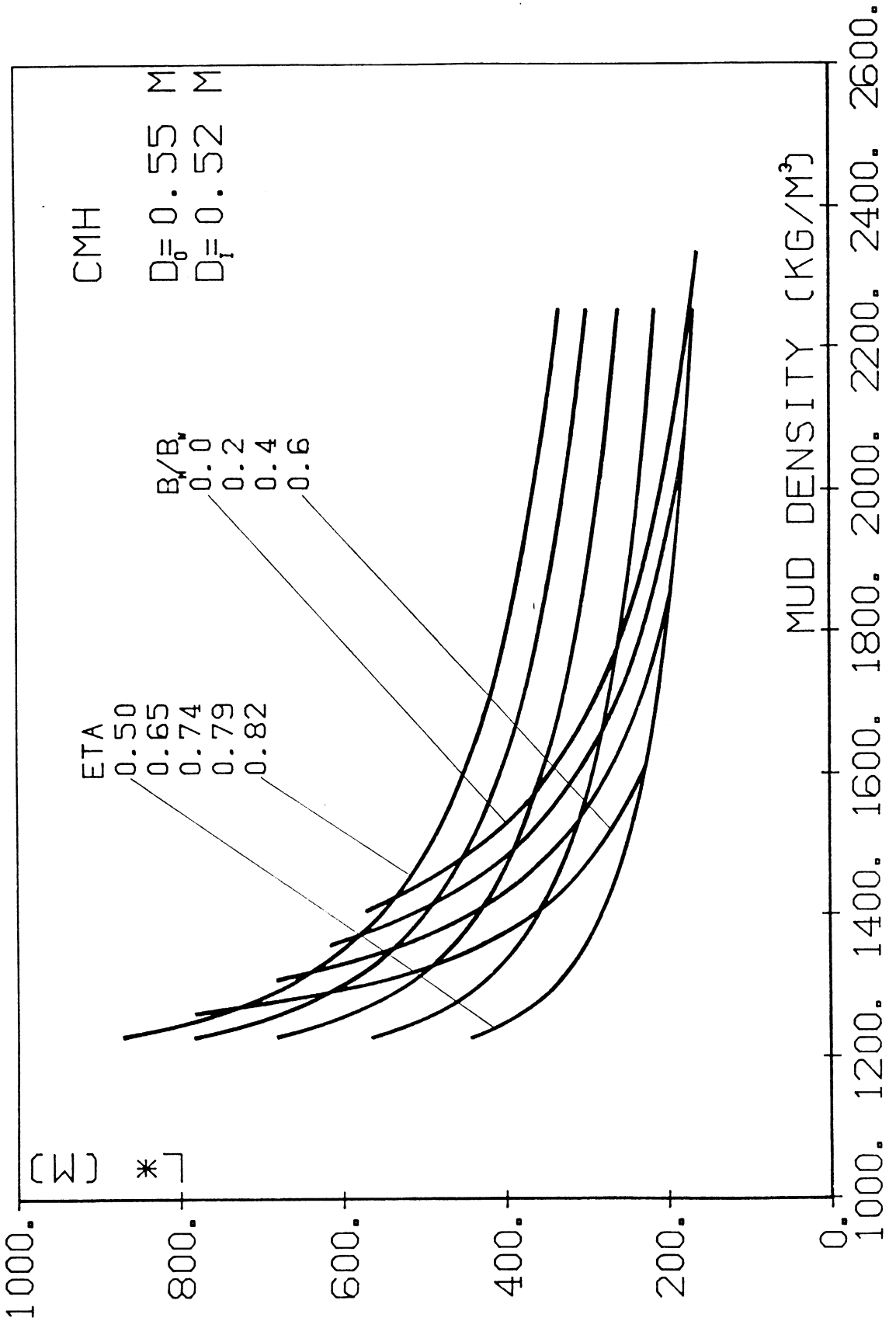

Figure 25. L* versus ρ_m for Clamped-Movably Hinged Risers for D_o = 0.55m and D_i = 0.515m

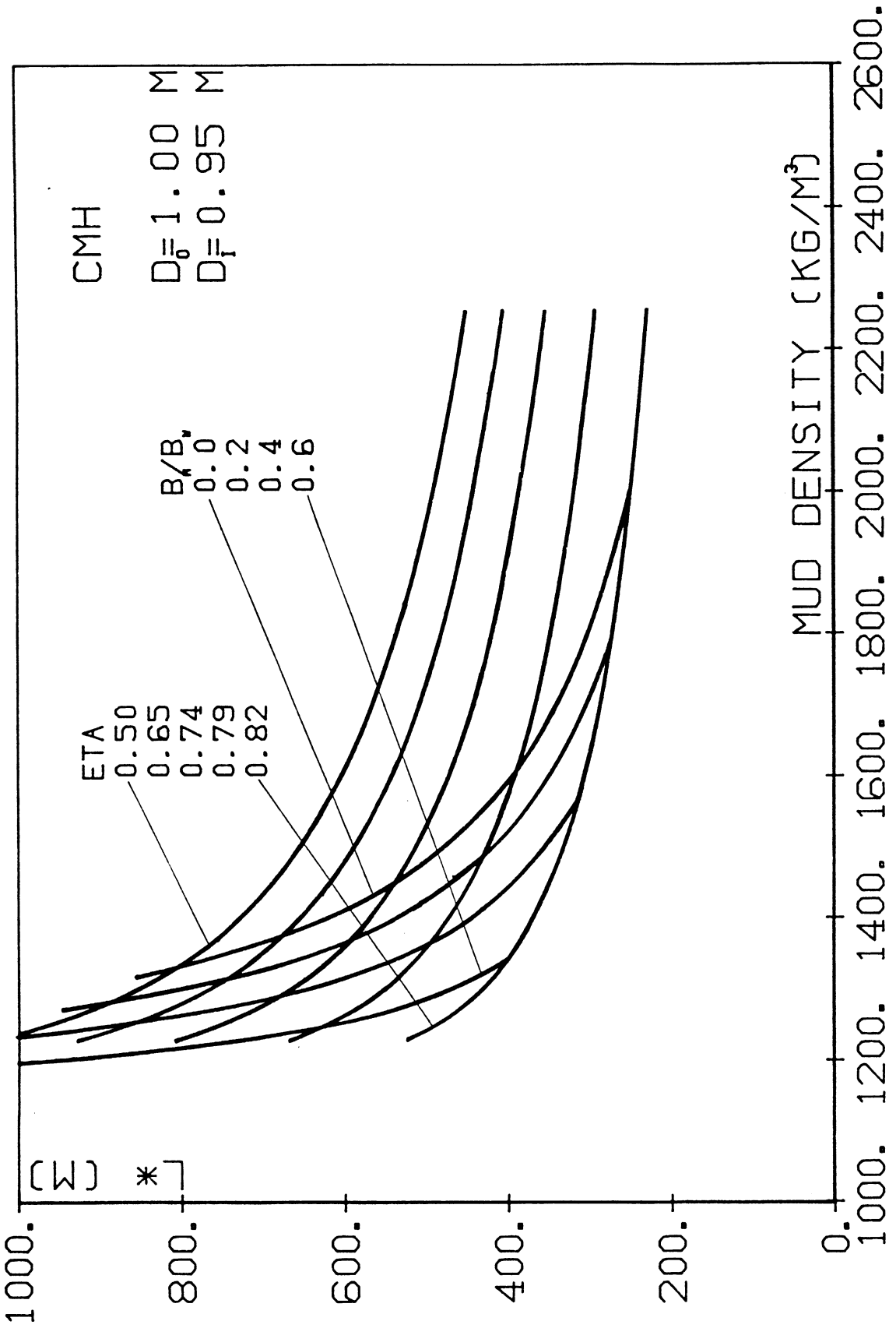

Figure 26. L* versus ρ_m for Clamped-Movably Hinged Risers for D_o = 1.00m and D_i = 0.95m

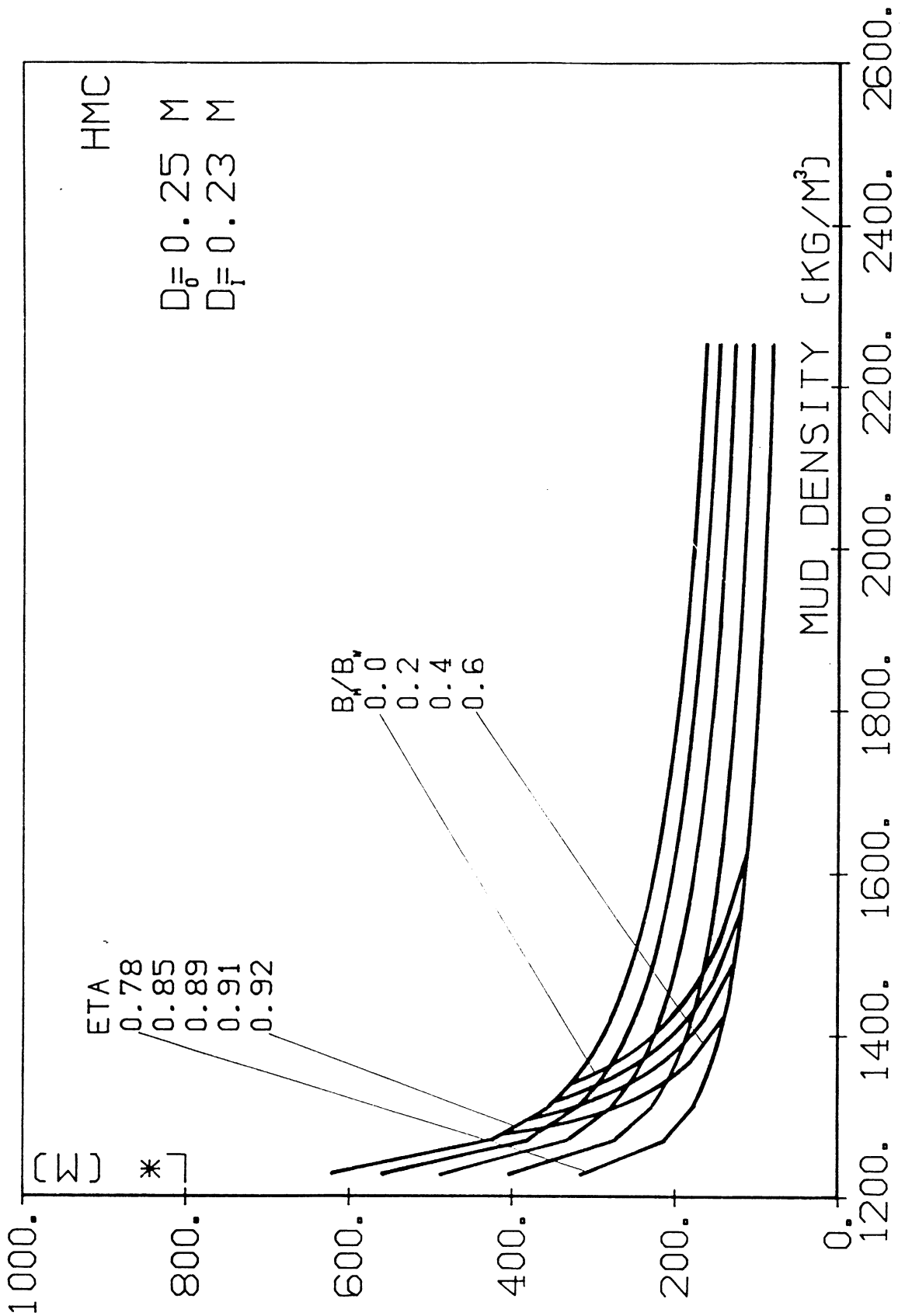

Figure 27. L* versus ρ_m for Hinged-Movably Clamped Risers for D_o = 0.25m and D_i = 0.23m

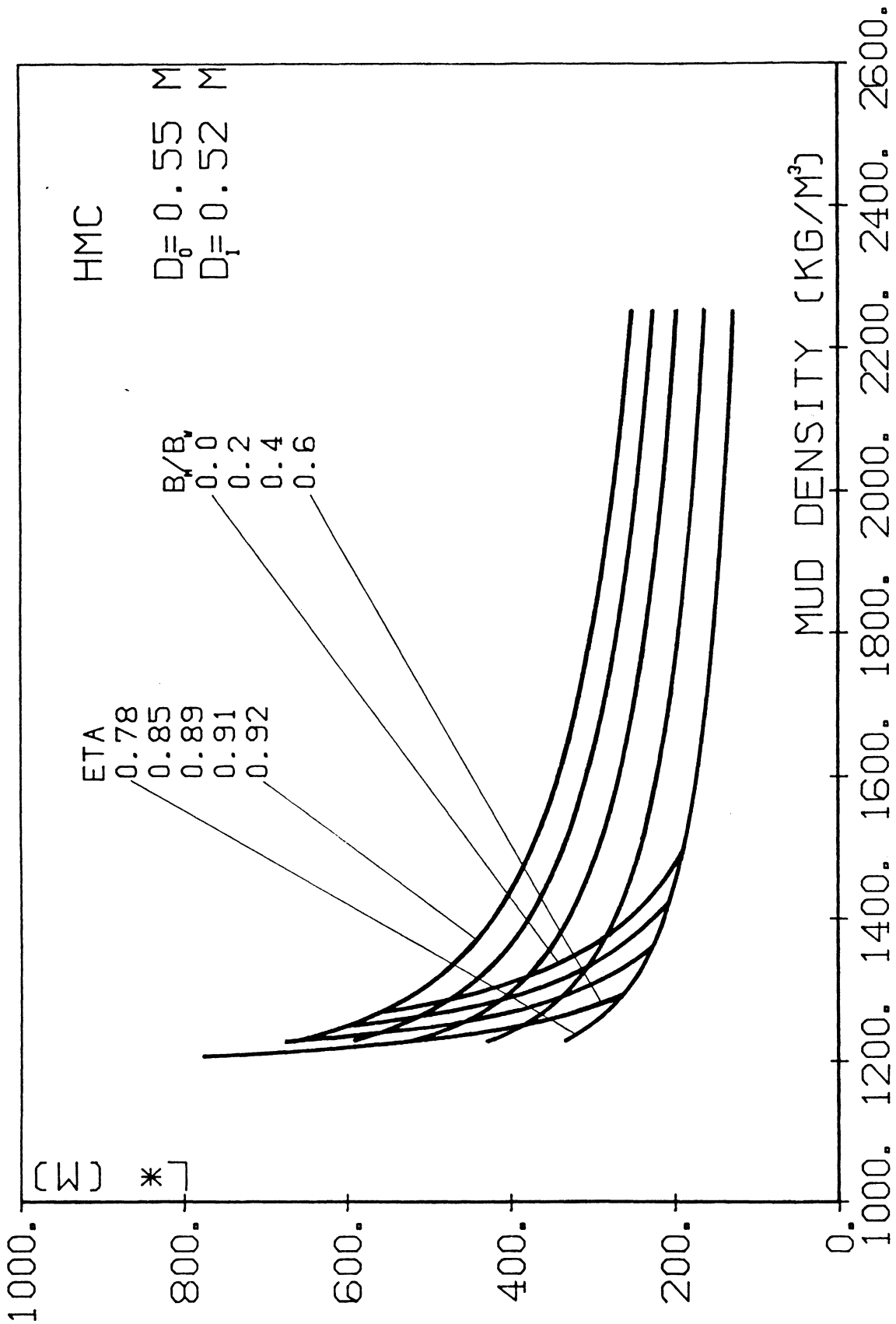

Figure 28. L* versus ρ_m for Hinged-Movably Clamped Risers for D_o = 0.55m and D_i = 0.515m

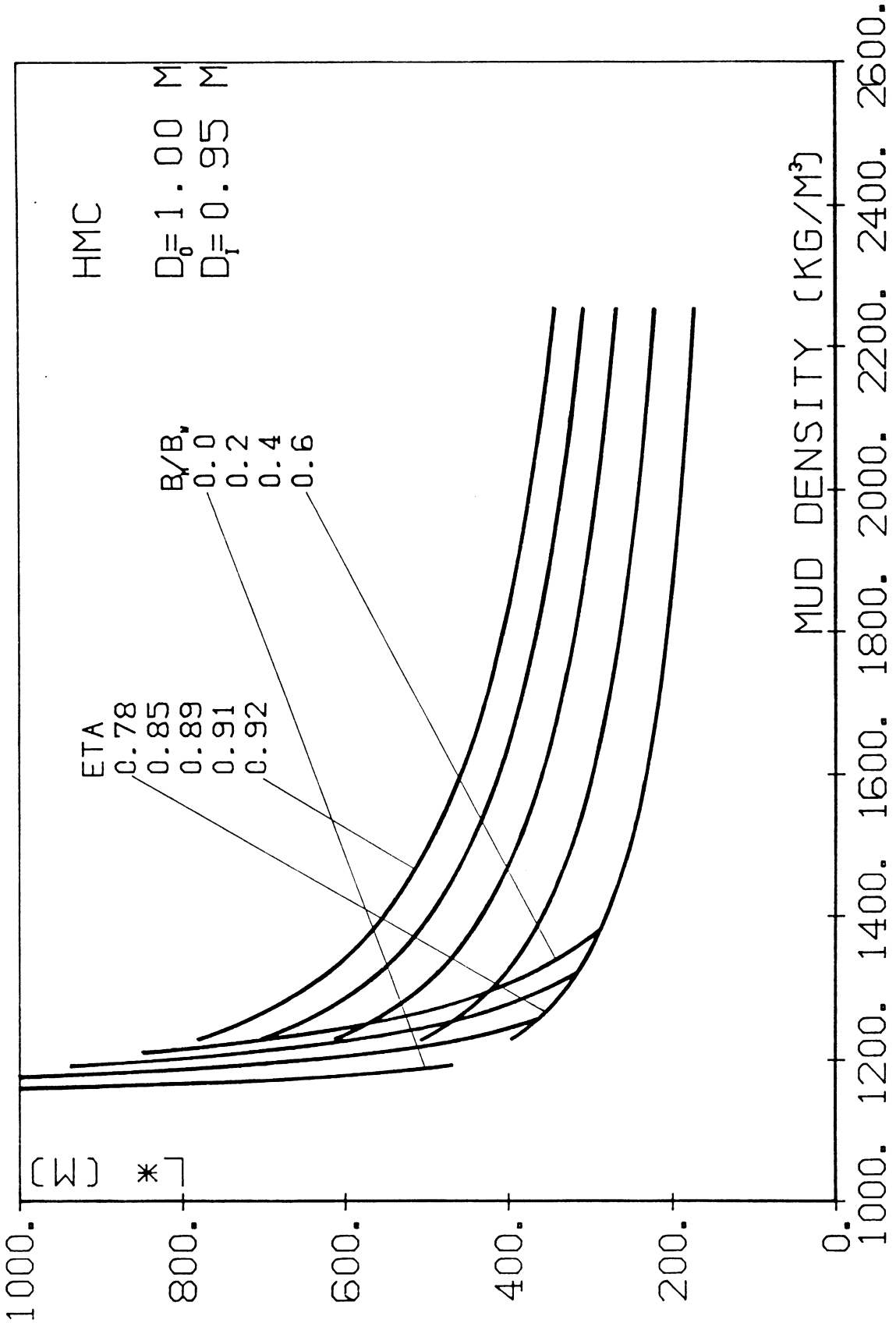

Figure 29. L* versus ρ_m for Hinged-Movably Clamped Risers for D_O = 1.00m and D_i = 0.95m

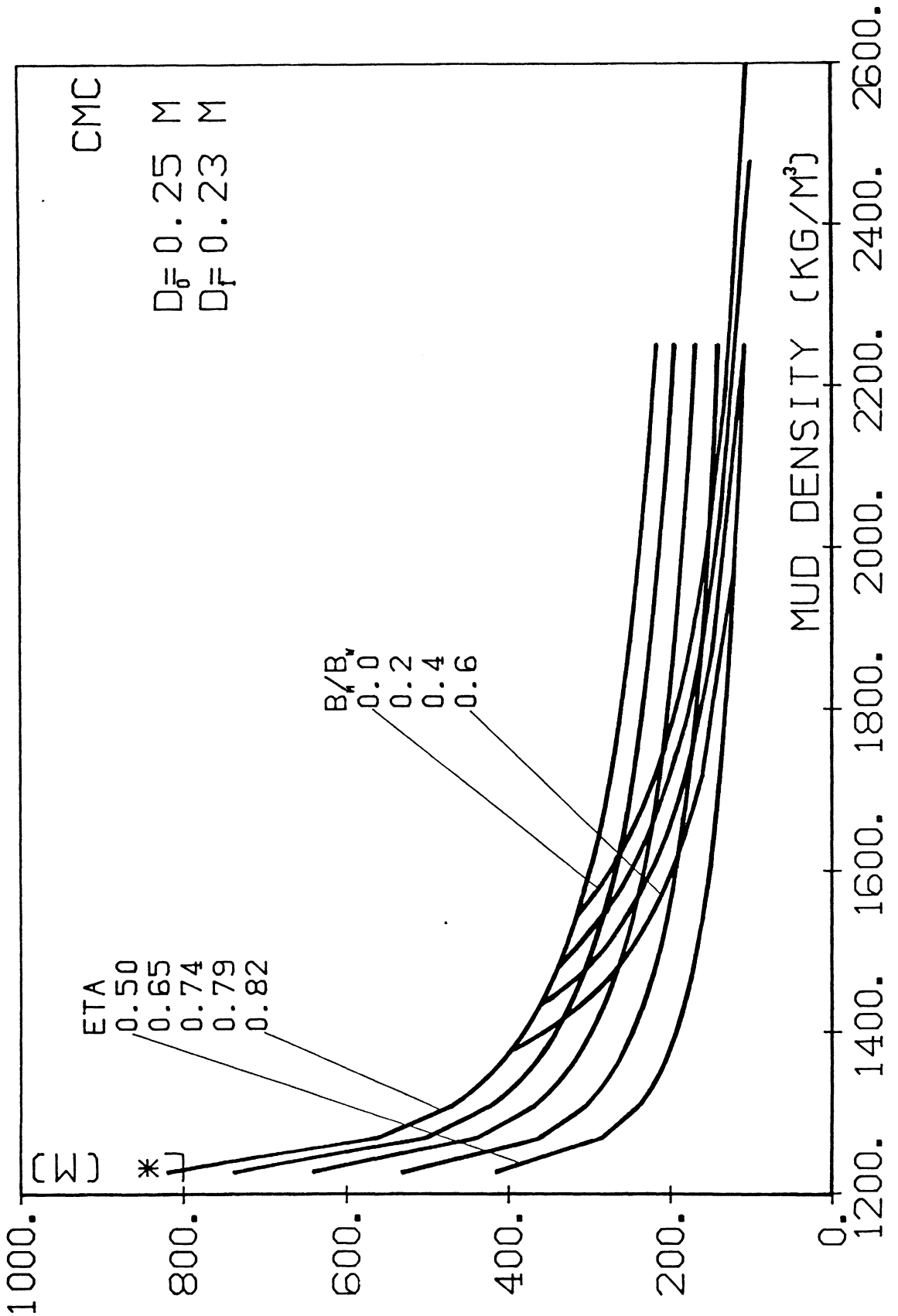

Figure 30. L* versus ρ_m for Hinged-Movably Clamped Risers for D_O = 0.25m and D_I = 0.23m

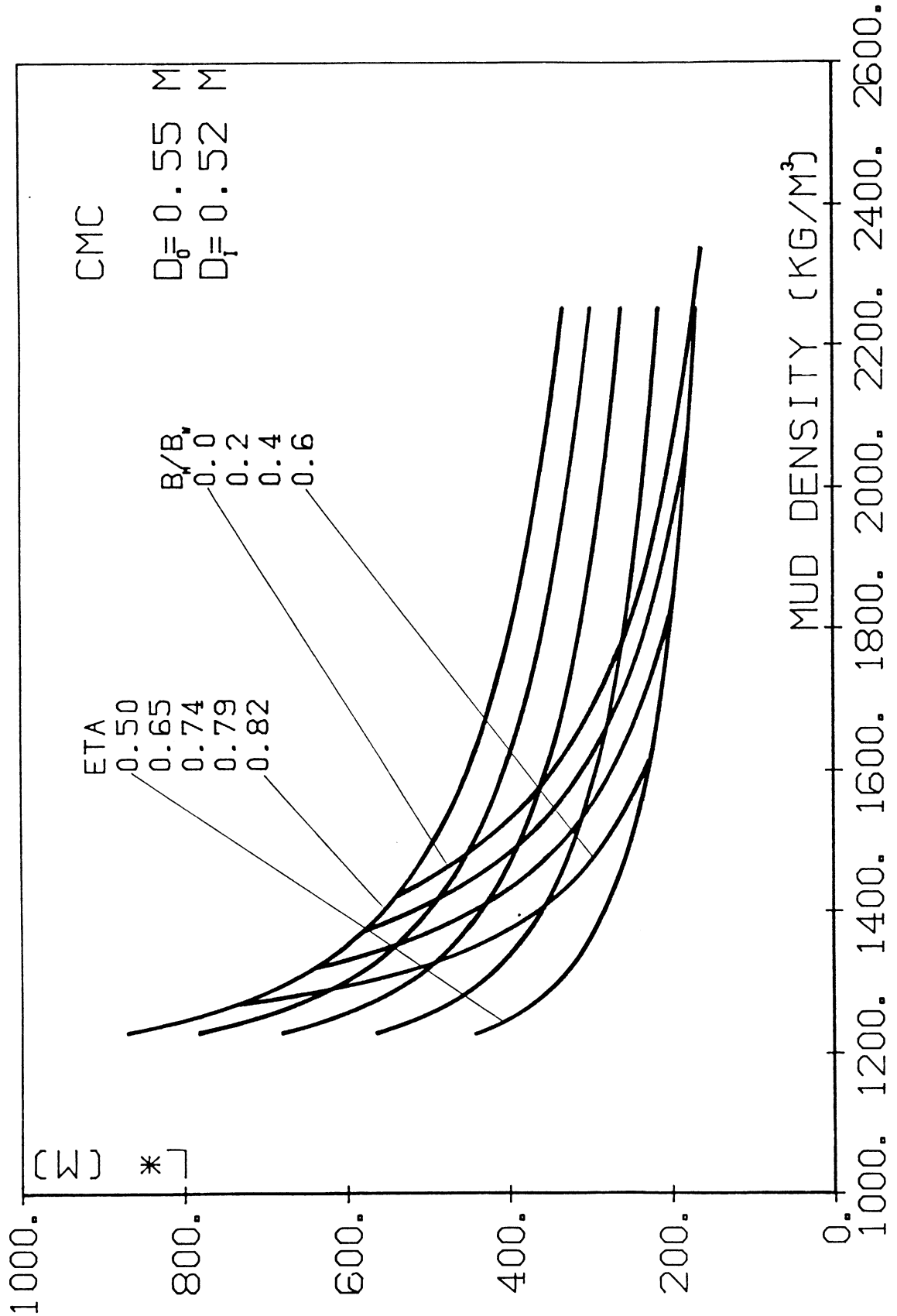

Figure 31. L* versus ρ_m for Hinged-Movably Clamped Risers for D_o = 0.55m and D_i = 0.515m

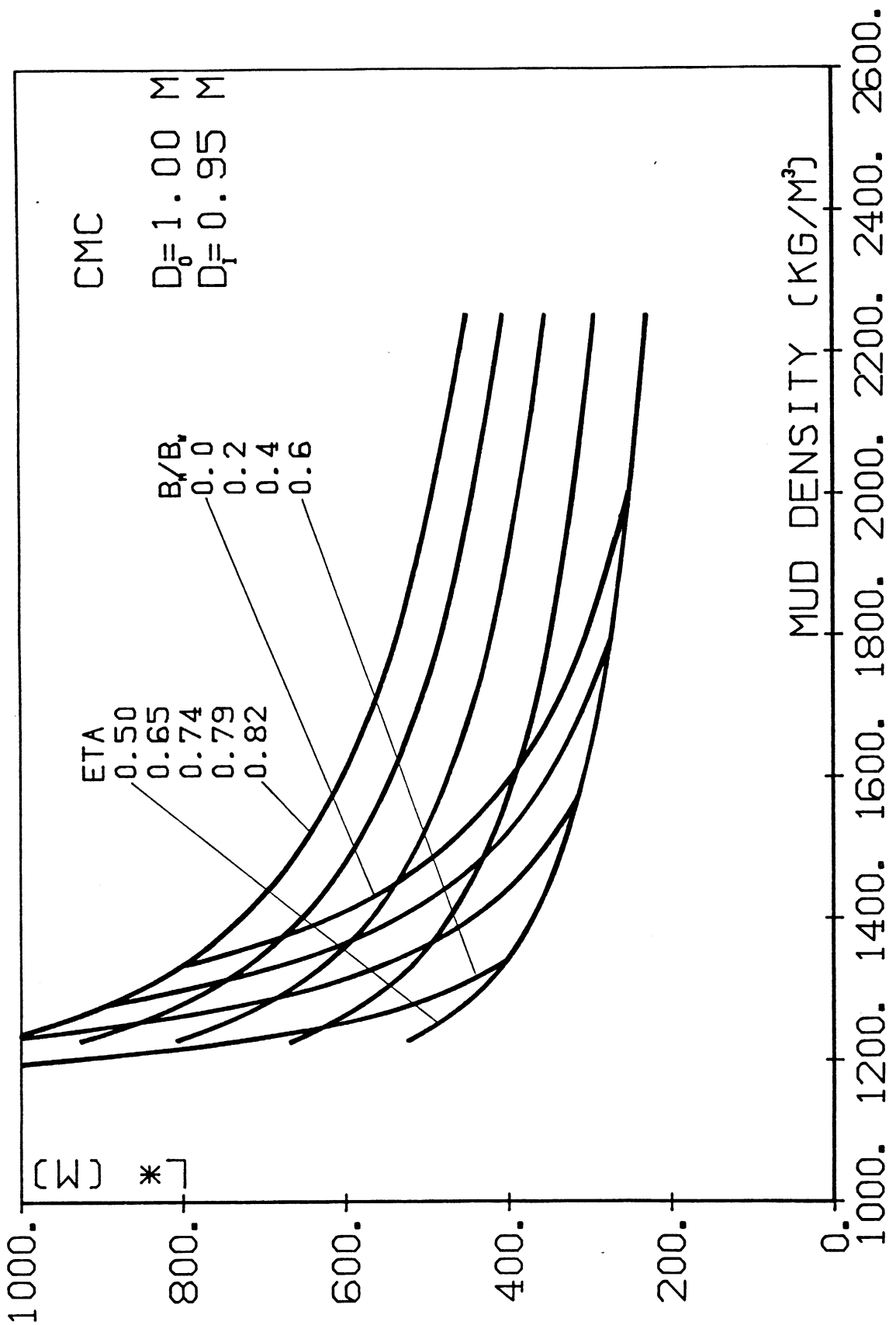

Figure 32. L* versus ρ_m for Hinged-Movably Clamped Risers for D_o = 1.00m and D_i = 0.95m

IV. COMPARISON OF CRITICAL LENGTH FOR RISERS WITH NONMOVABLE BOUNDARIES

To make the comparison of the critical length curves derived in Chapter III easier, in this Chapter we plot the critical length versus ρ_m curves in Figures 33, 34 and 35 for all three riser configurations, defined by equations (III-3) to (III-8), and for $B_m/B_w = 0.2$.

Each figure includes one curve for each set of boundary conditions for risers with nonmovable boundaries. These figures verify the conclusions derived in Section III.5. and in addition show that the effect of the lower boundary condition is more important than that of the upper one. Actually the critical length curves for hinged-hinged and hinged-clamped risers almost coincide and so do the corresponding curves for clamped-hinged and clamped-clamped risers. In fact for high values of L^* the curves are identical as can be deduced from the asymptotic behavior of riser stability boundaries derived in reference [9].

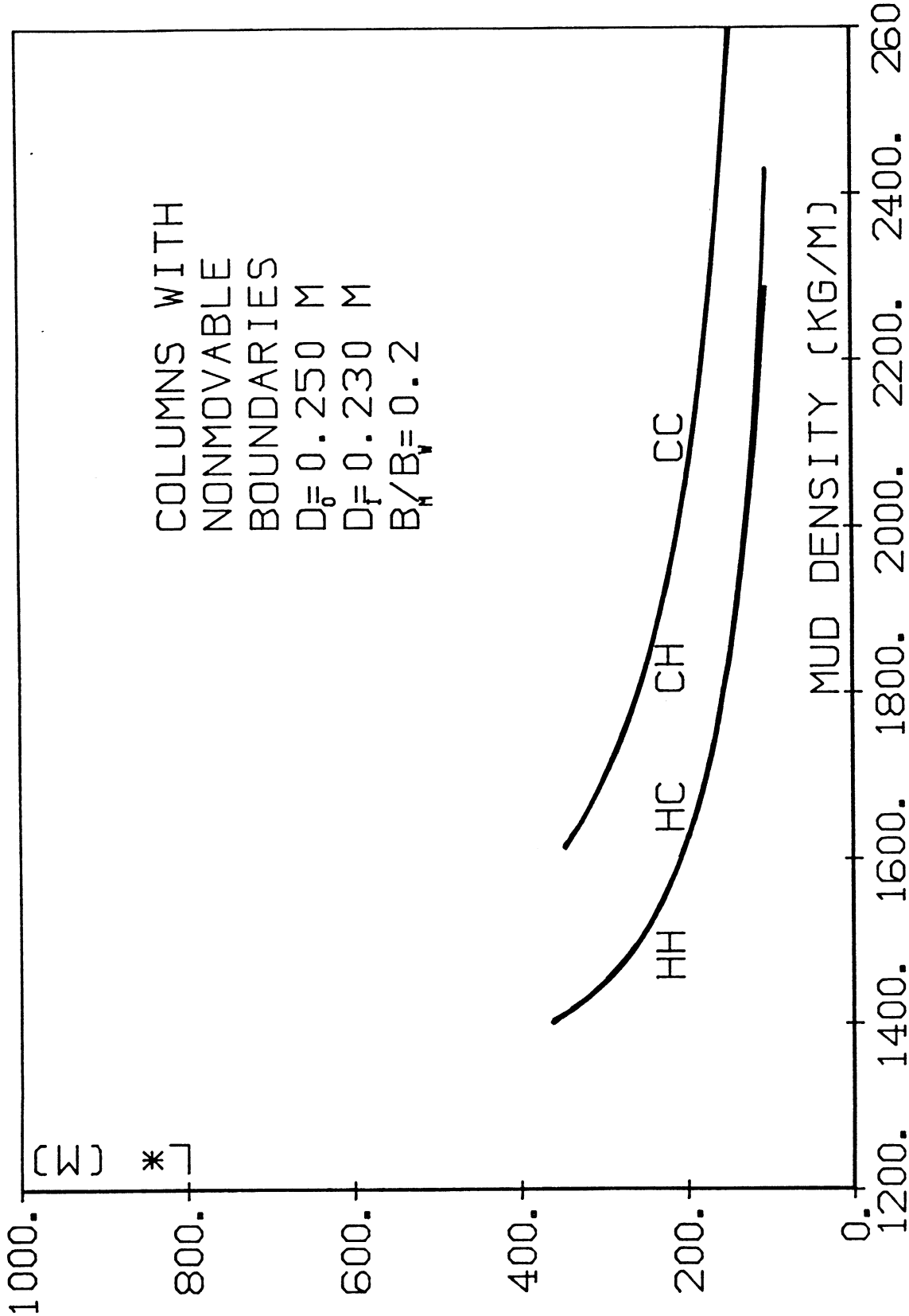

Figure 33. L* versus ρ_m for Risers with Nonmovable Boundaries for D_o = 0.25m, D_i = 0.23m and b_m/b_w = 0.2

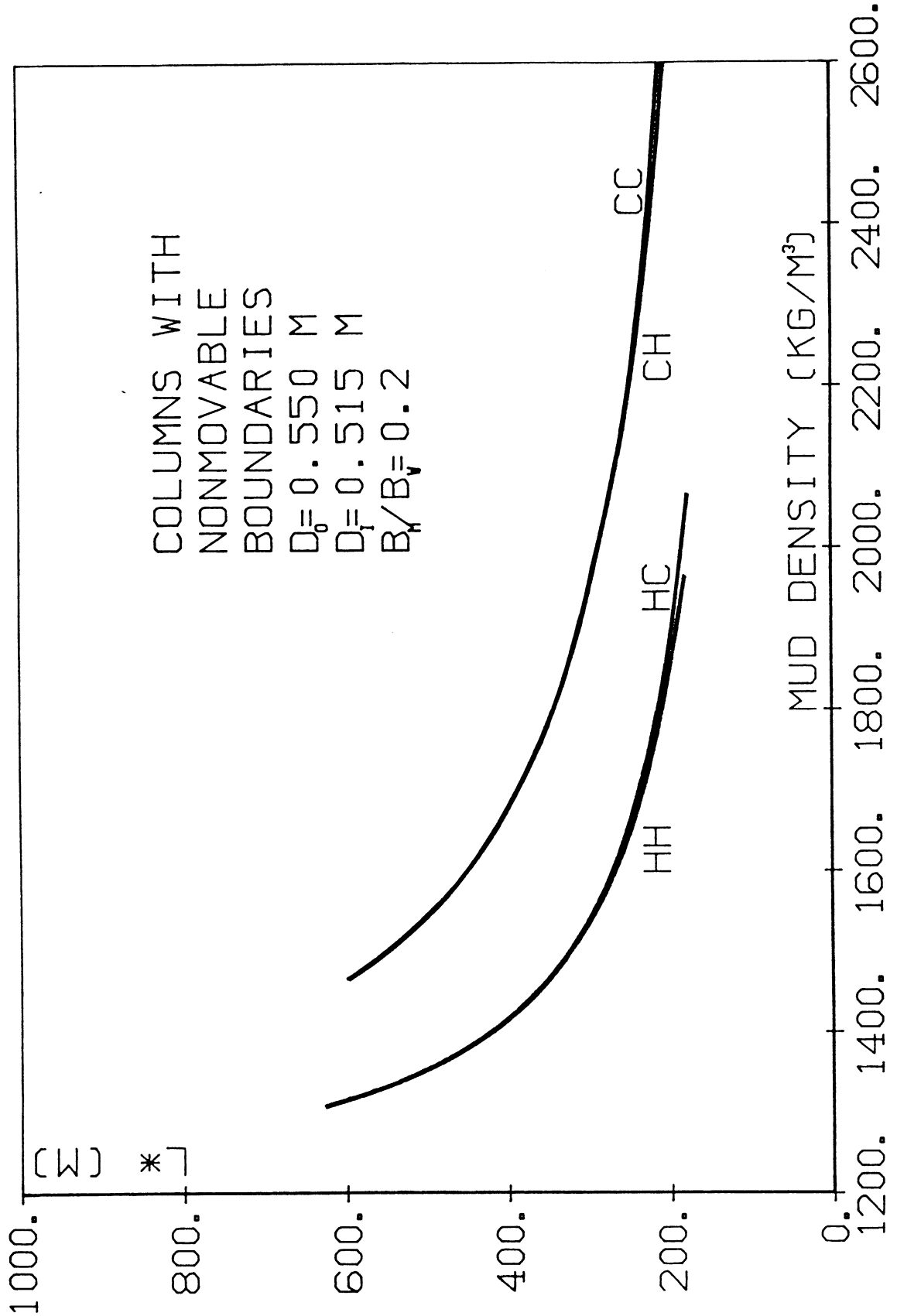

Figure 34. L* versus ρ_m for Risers with Nonmovable Boundaries for D_o = 0.55m, D_i = 0.515m and b_m/b_w = 0.2

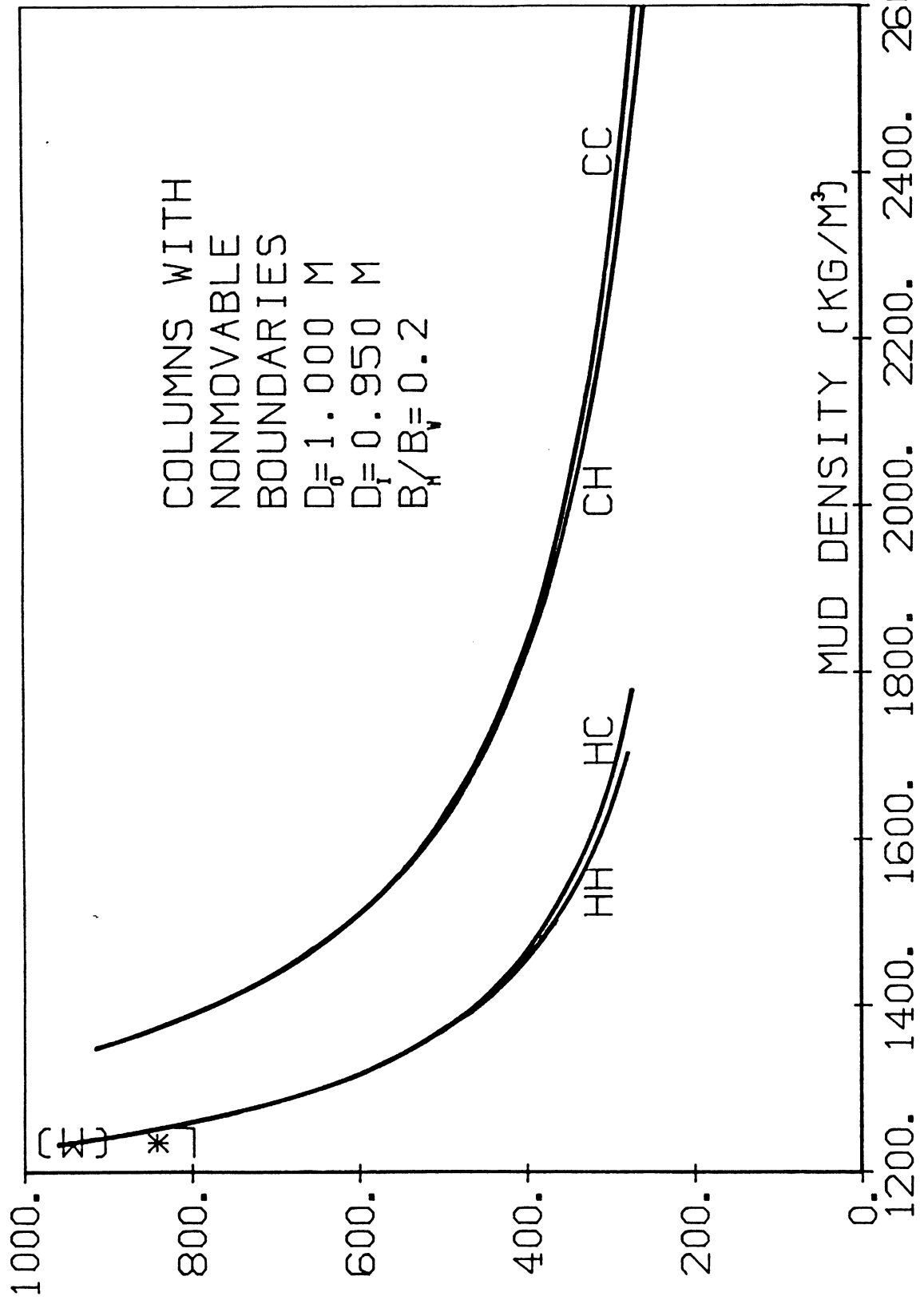

Figure 35. L* versus ρ_m for Risers with Nonmovable Boundaries for D_o = 1.00m, D_i = 0.95m and b_m/b_w = 0.2

V. COMPARISON OF CRITICAL LENGTH FOR RISERS WITH MOVABLE BOUNDARIES

Analysis similar to the one done in Chapter IV is repeated in this Chapter for risers with movable top supports and specifically for the four sets of boundary conditions considered in this work. The results are shown in Figures 36, 37 and 38 and verify the conclusions derived in Section III.9. In addition, as in the case of risers with nonmovable boundaries it is obvious that the effect of the lower end boundary condition is more important than that of the upper end condition. In all three figures, curves corresponding to risers with the same lower end boundary condition are identical. This can also be explained theoretically on the results of reference [9] which deals with the asymptotic behavior of riser stability boundaries.

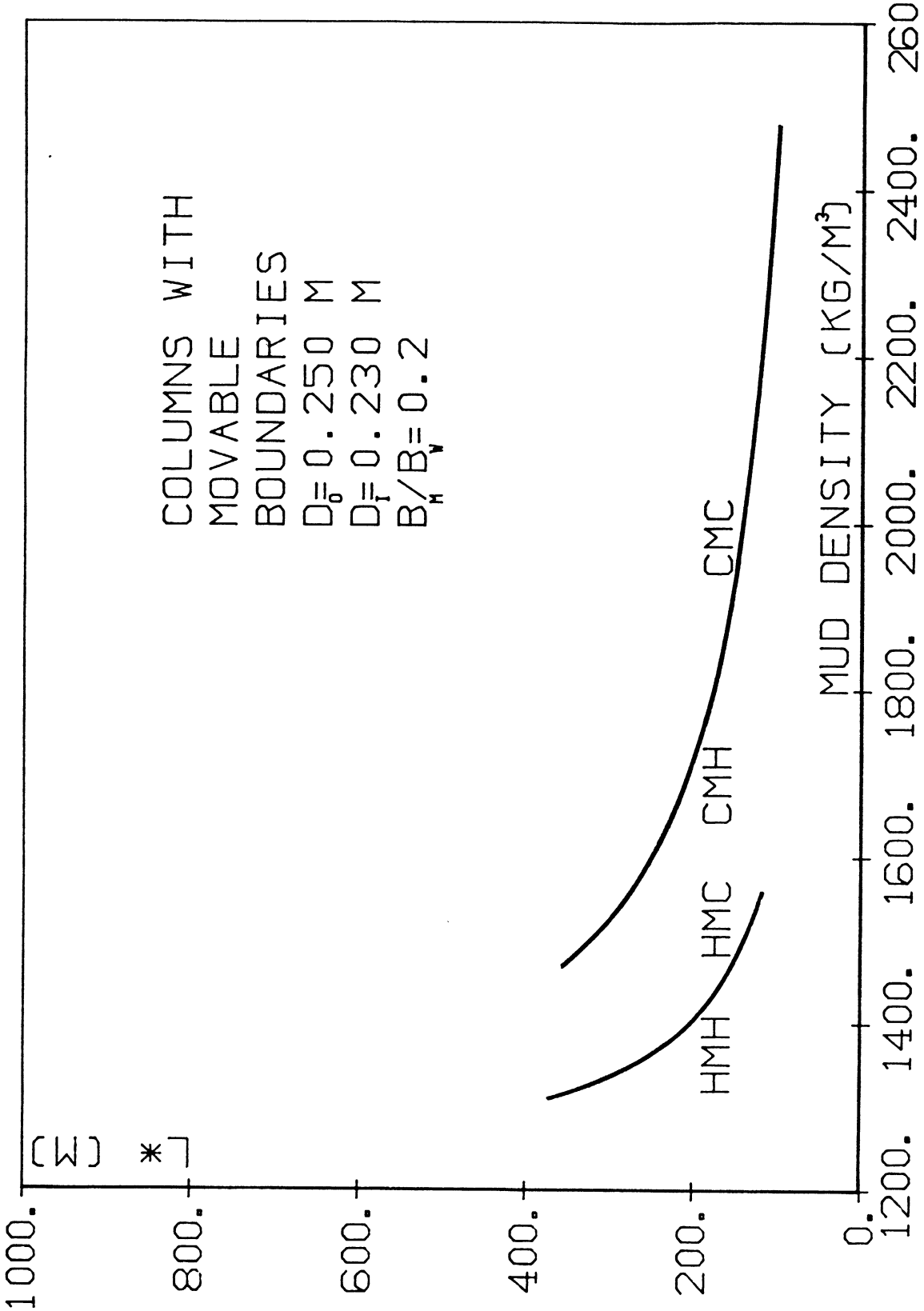

Figure 36. L* versus ρ_m for risers with Movable Boundaries for D_o = 0.25m, D_i = 0.23m and h_m/b_w = 0.2

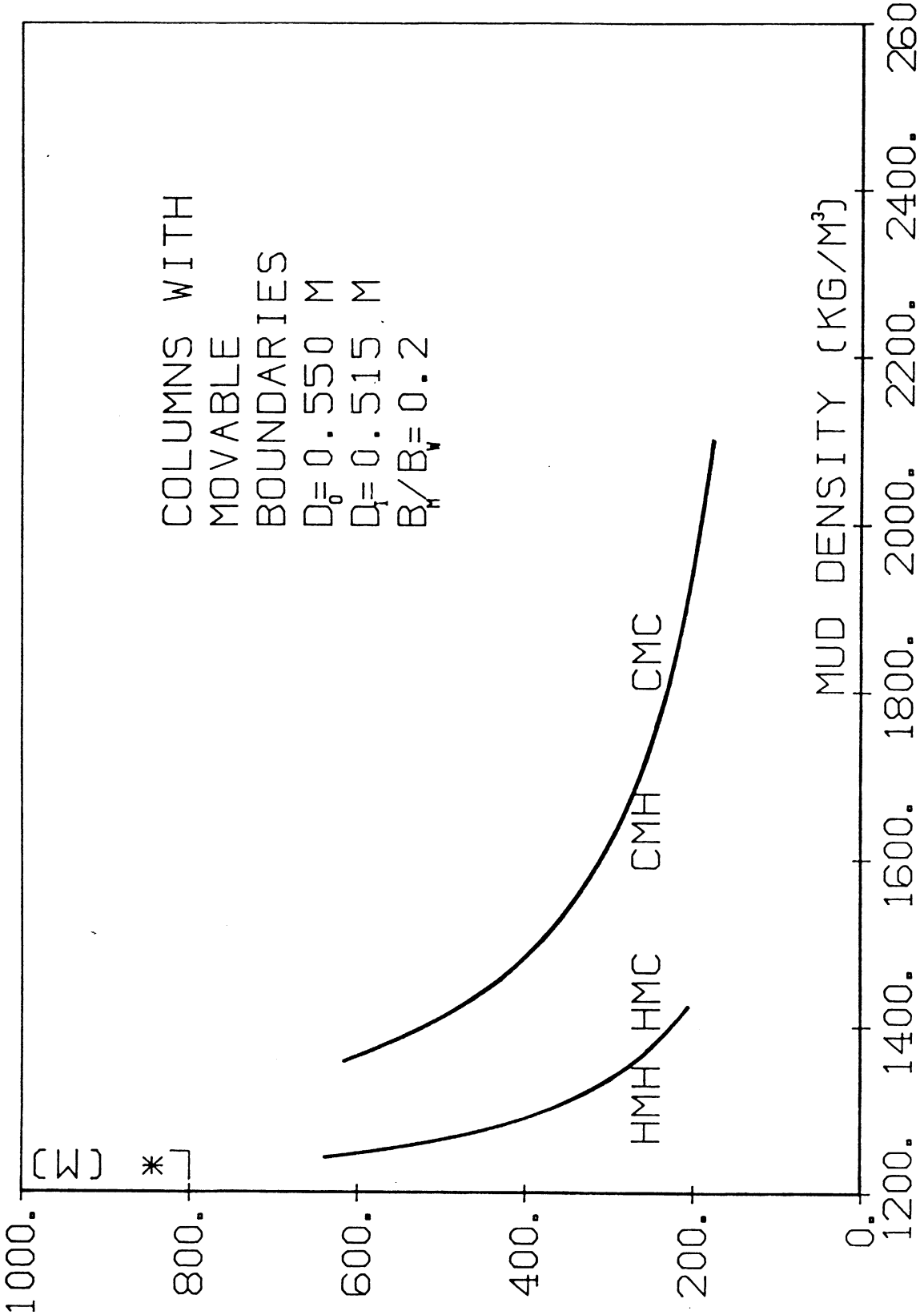

Figure 37. L* versus ρ_m for risers with Movable Boundaries for D_o = 0.55m, D_i = 0.515m and h_m/b_w = 0.2

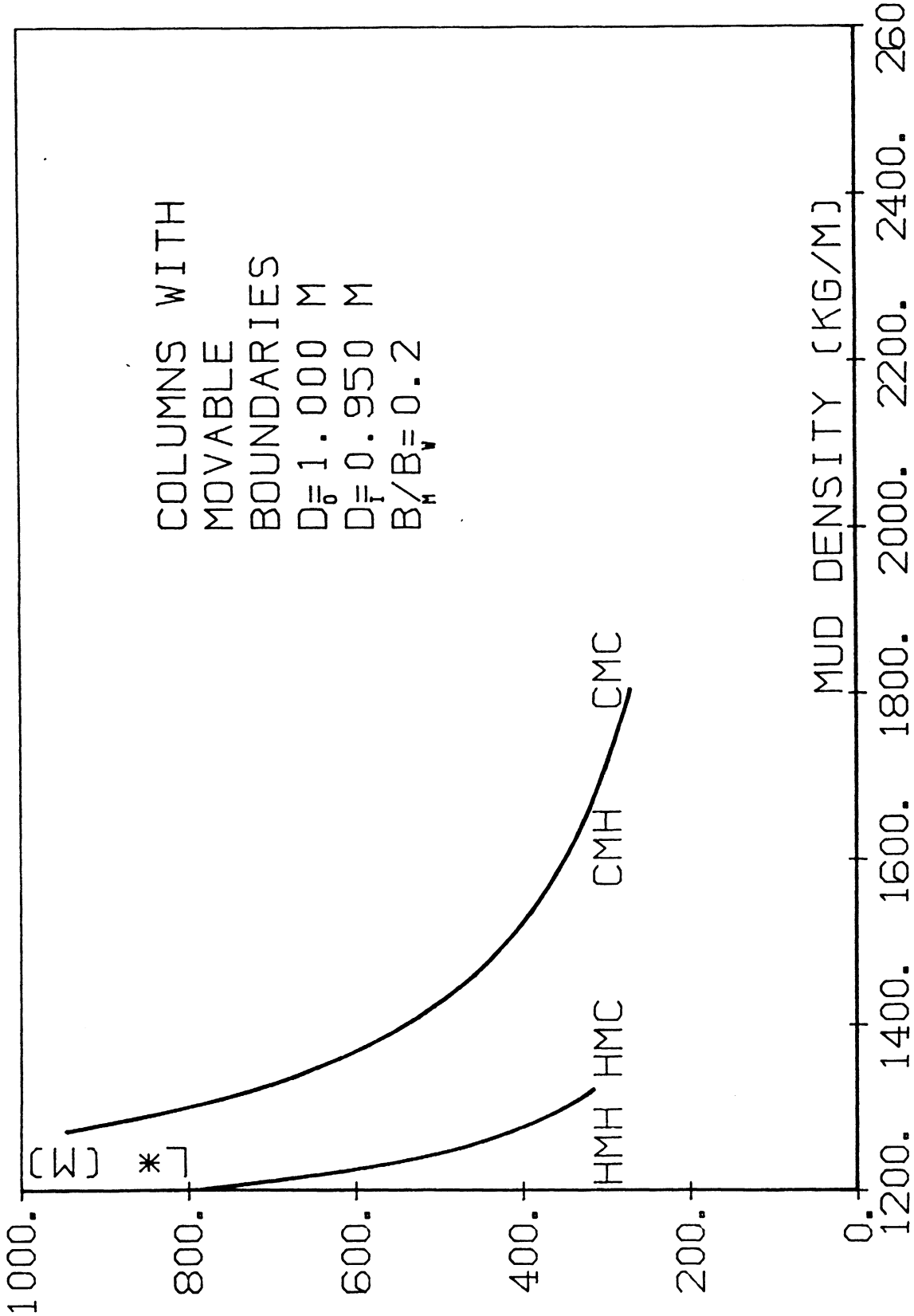

Figure 38. L* versus ρ_m for risers with Movable Boundaries for D_o = 1.00m, D_i = 0.95m and b_m/b_w = 0.2

SUMMARY

The stability boundaries of risers for eight different sets of boundary conditions have been derived in previous work [5,9]. In this report these results were used to prove that risers which are in tension along their entire length may buckle globally as Euler columns due to the action of internal fluid static pressure force.

Critical β value, β^*, which if exceeded may result in buckling in tension has been defined and computed for the eight sets of boundary conditions considered in this work.

Critical values of the riser length, L^*, corresponding to β^*, have been derived for typical risers and over wide ranges of the drilling mud density ρ_m and buoyancy supporting forces, B_m/B_w, showing that for typical designs, L^* is of the order of a few hundred meters. The dependence of L^* on the major riser properties and boundary conditions has also been studied. It has been shown that for a given type of top support, movable or nonmovable, the critical riser length, L^*, strongly depends on the lower end boundary condition and only weakly on the upper end one.

REFERENCES

1. Abramowitz, M. and Stegun, I.A., Handbook of Mathematical Functions, Dover, New York, 1970.

2. Bender, C.M., and Orszag, S.A., Advanced Mathematical Methods for Scientists and Engineers, McGraw-Hill Book Co., 1978.

3. Bernitsas, M.M., "Riser Top Tension and Riser Buckling Loads," ASME AMD, Vol. 37, November 1980, pp. 101-109.

4. Bernitsas, M.M., "Static Analysis of Marine Risers," Department of Naval Architecture and Marine Engineering, The University of Michigan, Report No. 234, June 1981.

5. Bernitsas, M.M., Kokkinis, T., and Faller, W., "Buckling of Slender Columns under Distributed Load," Department of Naval Architecture and Marine Engineering, The University of Michigan, Report No. 240, December 1981.

6. Bernitsas, M.M., "Problems in Marine Riser Design," Marine Technology, Vol. 19, Number 1, January 1982, pp. 73-82.

7. Bernitsas, M.M., "Three Dimensional, Non-Linear Large Deflection Model of Dynamic Response of Risers, Pipelines and Cables," Journal of Ship Research, Vol. 26, No. 1, March 1982, pp. 59-64.

8. Bernitsas, M.M. and Kokkinis, T., "Global Buckling Design Criteria for Risers," Proceedings of Conference on the Behavior of Offshore Structures, BOSS '82, Boston, Massachusetts, August 1982, pp. 705-715.

9. Bernitsas, M.M., and Kokkinis, T., "Asymptotic Behavior of Riser Stability Boundaries," Department of Naval Architecture and Marine Engineering, The University of Michigan, Report No. 255, December 1982.

10. Bernitsas, M.M., and Kokkinis, T., "Buckling of Risers in Tension due to Internal Pressure: Nonmovable Boundaries," Proceedings of the Second Offshore Mechanics and Arctic Engineering Symposium, ASME, February 1983, and Journal of Energy Resources Technology, (in press, 1983).

11. Bernitsas, M.M., and Kokkinis, T., "Buckling of Columns with Movable Boundaries," Journal of Structural Mechanics, (in press, 1983).

12. Biezeno, C.B. and Koch, J.J., "Note on the Buckling of a Vertically Submerged Tube," Applied Scientific Research, Sec. A., Vol. 1, No. 2, 1948, pp. 131-138.

13. Duncan, W.J., "Multiply and Continuously Loaded Struts," Engineering, Vol. 174, 1952, pp. 180-182.

14. Goodman, T.R. and J.S. Breslin, "Static and Dynamics of Anchoring Cables in Wakes," Journal of Hydronautics, Volume 10, No. 4, pp. 113-120.

15. Huang, T. and Dareing, D.W., "Buckling and Frequency of Long Vertical Pipes," Journal of Engineering Mechanics Division, Proceedings of the ASCE, Vol. 95, Feb. 1967, pp. 167-181.

16. Huang, T., and Dareing, D.W., "Buckling and Lateral Vibration of Drill Pipe," Journal of Engineering for Industry, Transactions ASME, Vol. 90, Nov. 1968, pp. 613-619.

17. Lubinski, A., "A Study of the Buckling of Rotary Drilling Strings," Drilling and Production Practice, API, 1950, pp. 178-214.

18. Morgan, G.W., "Force Systems Acting on Arbitrarily Directed Tubular Members in the Sea," Energy Technology Conference and Exhibit, Paper 77-Pet-38, Houston, Texas, Sept. 1977.

19. Plunkett, R., "Static Bending Stresses in Catenaries and Drill Strings," Journal of Engineering for Industry, Transactions ASME, Series B, Vol. 89, No. 1., February 1967, pp. 31-36.

20. Sherman, D.R. and Erzurumlu, H., "Behavioral Study on Circular Tubular Beam Columns," Journal of Structural Division, Proceedings of the ASCE, Vol. 105, STG, June 1979, pp. 1055-1068.

21. Sugiyama, Y. and Ashida, K., "Buckling of Long Columns under Their Own Weight," Transactions, Japanese Society of Mechanical Engineers, Vol. 21, No. 158, August 1978, pp. 1228-1235.

22. Willers, F.A., "Das knicken Schwerer Gestaenge," Zeitung fuer Angewandte Mathematik und Mechanik, Vol. 21, No. 1, 1941, pp. 43-51.